UNIVERSITÉ DU QUÉBEC À MONTRÉAL

SOURCES ET FACTEURS MENANT À LA SURSATURATION EN CO_2 DES RIVIÈRES BORÉALES

MÉMOIRE

PRÉSENTÉ

COMME EXIGENCE PARTIELLE

DE LA MAITRISE EN BIOLOGIE

PAR

MARIE LAURE GÉRARDIN

DÉCEMBRE 2019

REMERCIEMENTS

J'aimerais remercier toute l'équipe du CarBBAS et en particulier mon superviseur, Paul del Giorgio, sans qui cette aventure telle que je l'aie connue n'aurait jamais pu se produire. Merci au soutien constant, que m'ont apporté à la fois l'ancienne génération du groupe, à savoir, Carolina Garcia Chaves, Clara Ruiz Gonzalez, Terhi Rasilo, Tonya del Sontro et Matthew Bogard et la nouvelle génération tel que Cynthia Soueid, Felipe Rust, Julia Jakobsson, Tristy Vick-Majors, Sophie Crevecoeur qui ont tous participé de près ou de loin à ce projet. Sans oublier les membres du labo de Yves Prairie, Shoji Thottathil, Paula Reis et Ji-Hyeon Kim. Je tenais également à remercier toutes les personnes qui m'ont aidé dans la récolte des données, sur le terrain et en laboratoire, Annick St Pierre, Alice Parkes et Serge Paquet pour leur planification impeccable. Pour l'aide de terrain et de laboratoire et leur soutien infatigable quelque soit l'heure ou la météo, Martin Demers, Alexandre Ducharme, sans oublier le trio Brad, Chad and Chase. Mais tout ce travail n'aurait pas été possible sans l'apport, la patience, les conseils et le temps d'Erin Hotchkiss, qui m'a accueilli au sein de son groupe et de Joan Pere Casas Ruiz et Ryan Hutchins, qui ont tous deux su m'aider et me conseiller du début à la fin de ce projet de maîtrise. Un merci tout particulier à ma collègue, coloc, et amie Karelle Desrosiers avec qui j'ai partagé des journées et soirées à discuter de nos projets. Enfin, cette étude aurait été impossible sans le soutien du GRIL, des bourses de la Fondation UQÀM, ainsi que celle d'HydroQuébec (Projet *La Romaine*).

AVANT-PROPOS

Ce mémoire de maîtrise est réparti en quatre sections : une introduction générale présentant le contexte général de l'étude, deux chapitres sous forme d'article ainsi qu'une conclusion générale. Les articles sont rédigés en anglais, dans l'objectif d'être publiés. Le premier chapitre consistera en une revue de la littérature portant sur la caractérisation et la quantification des différentes contributions à l'émission de CO_2 des rivières boréales. Le second chapitre portera sur la reconstitution de la tendance au déclin de la pression partielle du CO_2 au sein d'un réseau hydrographique boréal.

Bien que les articles comportent des co-auteurs, ma contribution à ceux-ci demeure complète, en commençant par l'élaboration des concepts, de l'échantillonnage, l'analyse des données jusqu'à la rédaction. Ce document sera suivi d'une conclusion et d'une liste des références utilisées.

TABLE DES MATIÈRES

AVANT-PROPOS iv

LISTE DES FIGURES vii

LISTE DES TABLEAUX ix

LISTE DES ABRÉVIATIONS, DES SIGLES ET DES ACRONYMES x

LISTE DES SYMBOLES xi

LISTE DES UNITÉS xii

RÉSUMÉ xiii

ABSTRACT xv

INTRODUCTION 1

CHAPITRE I IDENTIFICATION ET LA QUANTIFICATION DES SOURCES ET PROCESSUS MENANT À LA SURSATURATION DES RIVIÈRES EN CO_2 4

1.1 Processus à l'origine de la sursaturation des milieux lotiques en CO_2 4

1.1.1 Sources de CO_2 4

1.1.2 Processus physiques influençant la sursaturation en CO_2 7

1.2 Émissions de CO_2 7

1.3 Variabilité spatiale dans les sources et les processus à l'origine des concentrations et des flux de CO_2 des cours d'eau 9

1.4 Variabilité temporelle des sources et processus à l'origine des concentrations et des flux de CO_2 dans les cours d'eau 10

1.5 Objectifs et hypothèses 12

1.6 Approche utilisée 16

CHAPITRE II UNDERSTANDING THE PROCESSES UNDERLYING THE PATTERN OF pCO_2 DECLINE ALONG A RIVERINE CONTINUUM 18

2.1. Abstract 18

2.2. Introduction 19

2.3. Material and methods 23

2.3.1. General approach: a quantitative framework 23
2.3.2. Site information and context 23
2.3.3. Sampling protocol, frequency and analytical methods 26
2.3.4. Assessing the influence of each process to stream CO_2 dynamics along a fluvial network 31

2.4. Results 34

2.4.1. General stream conditions 34
2.4.2. Network patterns of measured processes and fluxes 36
2.4.3. Test of the combination of fluxes to reconstruct the stream k_{600} along the fluvial network of *La Petite Romaine* 40
2.4.4. Contribution of different pathways to CO_2 dynamics 43

2.5. Discussion 47

2.5.1. Network patterns in stream processes 47
2.5.2. Mass balancing k_{600} along the fluvial continuum 51
2.5.3. Influence of the various processes to the fluvial CO_2 dynamics 54

2.6. Acknowledgements 56

APPENDICE A Supplementary methods 57

A.1 Water isotopes 58

A.2 Gas emissions, f_e 59

A.3 Lateral water inputs, Q_L 60

A.4 Stream metabolism and internal production of CO_2, f_m 61

APPENDICE B General framework 68

CONCLUSION 76

BIBLIOGRAPHIE 78

LISTE DES FIGURES

Figure 1.1 Sources et processus menant à l'émission de CO_2 des rivières : (1) minéralisation de la matière organique terrestre (OM) et transfert du CO_2 des sols vers la colonne d'eau, (2) minéralisation des matières organiques dissoute (DOC) et particulaire autochtone au sein de la colonne d'eau, (3) oxydation du CH_4 terrestre puis transfert vers la colonne d'eau et oxydation du CH_4 autochtone au sein de la colonne d'eau.

Figure 1.2 Graphique représentant les variations spatiales (gauche vers la droite = de la source vers les rivières plus larges) des pressions partielles en CO_2 (en µatm) de rivières localisées dans plusieurs régions du Québec.

Figure 1.3 Schéma représentant la variation attendue des divers flux (d'apports ou de pertes de CO_2) impliqués dans la sursaturation et la diminution en CO_2 des rivières au sein d'un réseau hydrographique. Ce réseau, aussi appelé « continuum fluvial », est découpé en tronçon représentant chacun une section de la rivière de l'amont A) vers l'aval B).

Figure 1.4 Représentation schématique d'un segment théorique de rivières, bordé des sections A (amont) et B (aval). Chacun des flux (*f*) sont représentés par des flèches, soit entrante dans le cas d'un flux positif, soit sortante dans le cas d'un flux négatif.

Figure 2.1 Location of *La Petite Romaine* stream network in la Côte Nord, Québec.

Figure 2.2 Seasonal and spatial stream pCO_2 (µatm) variability across the fluvial network of *La Petite Romaine,* ranging in size from headwaters to stream of strahler order 5 (from left to right).

Figure 2.3 Spatial and seasonal soil water contributions to the stream channel of: *a)* soil water pCO_2 (µatm), *b)* soil water DOC concentrations (mg C L^{-1}), *c)* lateral water input per kilometer length of stream (k_L, km^{-1}) and *d)* stream d-excess (‰) as a function of distance from headwaters (= 0 km) to larger streams.

Figure 2.4 Spatial distribution of the gas transfer velocity (k_{600}, m d^{-1}) estimated using 4 different methods, from left to right: a) CO_2 mass balance, b) floating chambers (average values over 2 years: 2015-2016), c) empirical equation of Natchimuthu et al., 2017, empirical equation n°6 Raymond et al., 2012 and Ulseth et al., 2019.

Figure 2.5 Contribution ratio of each flux (NEP, soil water inputs and emissions to the atmosphere) to the change in stream CO_2 flux within each segment, *i.e.* from theoretical upstream to downstream sites (A to B). This is the output plot of the mass balance.

Figure 2.6 Sources and contribution rate per meter length of stream to the stream CO_2 transported downstream declining pattern along a stream-river continuum.

Figure A.1 Log linear regression models based on measured stream water discharge (m^3 s^{-1}) and flow accumulation (pixel, using ArcGIS tool), for both spring and summer hydrological seasons, averaged for 2015 and 2016.

Figure A.1 Time series of the stream net ecosystem production (NEP, g C m^{-2} d^{-1}) in sites 2a and 2b, represented here as -NEP.

Figure A.3 Internal metabolism estimates for each segment, based on 2 methods: *1)* diurnal O_2 shifts (red dots in the 1st and 2nd segments) and *2)* DOC subtraction between soil and stream systems following Rasilo et al., 2017 (box plots).

LISTE DES TABLEAUX

Table B.1 Synthesis table of calculated fluxes based on empirical measurements (segments 1 to 4, from Strahler order 2 to 5). For each one of the 4 segments, values represent averages over 2 years, *i.e.* 2015-2016 and across the 2 sites together delimiting a segment (± standard error).

Table B.2 Comparison between gas transfer velocities (k_{600}, in m d^{-1}) obtained through a mass balance approach and the gas transfer velocities derived from empirical measurements (floating chambers), and empirical models found in the literature. The k_{600} calculated from equations in Ulseth et *al.,* 2019 and Natchimuthu et *al.,* 2017 represent both similar streams conditions to our, *i.e.* in small boreal streams. While the third empirical model is a global model applied on headwater streams (equation 6, Raymond et *al.,* 2012).

Table B.3 Table summarizing the main variables collected in *La Petite Romaine* stream (above) and soil water (below). Each column represents a different segment number in a growing stream order sequence, from left to right: Seg# 1 < 2 < 3 < 4.

LISTE DES ABRÉVIATIONS, DES SIGLES ET DES ACRONYMES

C Carbone

DIC Carbone Inorganique Dissous (Dissolved Inorganic Carbon)

DOC Carbone Organique Dissous (Dissolved Organic Carbon)

ER Ecosystem Respiration

GPP Gross Primary Production

IPCC Intergovernemental Panel on Climate Change

NEP Net Ecosystem Production

nLL negative Log Likelihood

PAR Photosynthetically Active Radiation

SD Standard Deviation

SE Standard Error

LISTE DES SYMBOLES

CO_2 Dioxyde de carbone

CH_4 Méthane

^{18}O, ^{2}H Isotopes stables de l'eau

d-excess Excès de deutérium

$\partial^{n}X$ Ratio isotopique (‰)

fx Flux (g C m^{-2} d^{-1})

f_s Apport latéral de CO_2 des sols vers la rivière

f_e Flux d'émission de CO_2 vers l'atmosphère

HCO_3^- Ions bicarbonates

k_{600} Coefficient d'échange gazeux eau - atmosphère (m d^{-1}) normalisé à 20°C

k_{CO_2} Coefficient d'échange gazeux eau - atmosphère (m d^{-1})

O_2 Dioxygène

pH Potentiel hydrogène

p*X* Pression partielle du gaz considéré X (µatm)

Q*x* Débit du cours d'eau (m^3 s^{-1})

w Largeur du cours d'eau (m)

x Longueur du segment de cours d'eau (m)

z Profondeur du cours d'eau (m)

LISTE DES UNITÉS

µatm	unité de pression, micro-atmosphère
m d^{-1}	unité du coefficient d'échange gazeux (*k*),
g m^{-2} d^{-1}	unité de flux, gramme de C ou O_2 par unité de surface par jour
g C m^{-3}	unité de concentration, gramme de C par unité de volume d'un mètre cube
mg L^{-1}	unité de concentration, milligramme par litre
mol L^{-1}	unité de concentration, mole par litre
m^3 s^{-1}	débit de rivière, volume d'un mètre cube par seconde
m^3 m^{-1} s^{-1}	débit d'entrée d'eau latérale (m^3 s^{-1}) par mètre de rivière
km^{-1}	contribution d'une variable donnée sur un segment de 1 km de rivière
µS cm^{-1}	unité de conductivité, micro-Siemens par centimètre
µmol photons m^{-2} d^{-1}	unité représentant les radiations photosynthétiques actives (PAR) par unité de surface par jour

RÉSUMÉ

Les rivières boréales sont d'importantes composantes du cycle global du carbone, révélant des concentrations en CO_2 plus élevées que l'atmosphère, de sorte à devenir des écosystèmes émetteurs de C. Malgré l'inhérente complexité des rivières de par leur hétérogénéité spatio-temporelle, à laquelle s'ajoute l'importante variabilité des rivières étudiées choisies dans la littérature, une tendance récurrente est tout de même observée, celle d'un déclin des concentrations en CO_2 des rivières de tête de bassin vers celles d'ordre plus élevé. De cette observation, découle plusieurs hypothèses toutes basées sur la mesure d'un processus en particulier à partir duquel les autres sont ensuite calculés, et ce, sans les confronter les uns avec les autres. Faire l'état des connaissances sur les sources et mécanismes responsables de l'enrichissement en CO_2 des rivières et de ces variations constitue le sujet de mon premier chapitre. Les ruisseaux et rivières de tête bénéficient de l'apport direct de CO_2 terrestre en lien avec leur étroite connexion avec les sols. Ensemble, les intrants de l'écosystème terrestre environnant et l'activité métabolique se produisant au sein du système aquatique sont reconnus comme étant à l'origine de la sursaturation en CO_2 des rivières. Pourtant, leur contribution relative est sujette à de nombreux débats dans la littérature. Bien que la majorité des études associe la perte de sursaturation des rivières avec la diminution de connexion des ruisseaux avec les sols, d'autres soulignent l'importance du processus de minéralisation de la matière organique. Dans le second chapitre, nous tentons de comprendre la tendance au déclin en pCO_2 des rivières au sein d'un continuum fluvial, en estimant chacun des flux impliqués ainsi que les variables les influençant, de manière individuelle et multiple (différentes méthodes). Ainsi, en utilisant le cas d'étude de La Petite Romaine (Nord du Québec), il nous sera permis de comparer nos attentes à la réalité, pour ensuite intégrer chacun des flux au sein d'un bilan de masse. Après quoi, la fermeture de ce bilan, nous donne des indications sur la compréhension de chacun des processus, et révèle les incertitudes et processus non considérés car non compris. Notre budget C, intégrant la contribution de chacun des facteurs de façon individuelle, révèle que les apports latéraux d'eau souterraine et de C contribuaient à environ 88 % au support des émissions de CO_2 au sein des plus petites rivières. Cet apport relatif diminuait progressivement à mesure que le volume des rivières augmentait. En contrepartie, le métabolisme interne à la rivière qui se trouvait initialement faible dans les petites rivières de haut de bassin, est progressivement devenu un contributeur essentiel responsable de la sursaturation des rivières d'ordres 4 à 5 (40%). Bien que le taux métabolique soit resté constant dans la rivière tout au long du continuum, c'est en réalité sa contribution relative, concomitante à la baisse substantielle des apports d'eau

latéraux, qui s'avérait donc augmenter. C'est en intégrant ces facteurs au sein d'un bilan de masse, qu'il nous a donc été possible de tester leur combinaison. Fermer ce bilan de masse nous indique donc que toutes les variables initialement testées et dont le caractère spatial individuel ne s'avérait pas concluant, sont toutes importantes et toutes requises pour expliquer le déclin de pCO_2. Ainsi, les débats tentant d'établir la variable responsable de cette diminution ne seraient alors pas fondés, puisqu'il s'agit en fait d'une combinaison de facteurs, propre au système considéré. Cette étude renforce l'importance de l'estimation de chacun des flux individuellement et leur comparaison pour la compréhension et l'estimation à plus grande échelle (spatiale et temporelle) des émissions de CO_2 lotique.

Mots clés : *déclin, continuum, métabolisme, apports latéraux, coefficient d'échange gazeux*

ABSTRACT

The emission of CO_2 from lotic systems is now recognized as a substantial flux of the global carbon (C) budget. Carbon dioxide can be produced either externally in soils or in situ within rivers column through various processes. Due to the scarcity of studies directly quantifying the absolute contributions of pathways of CO_2 along river networks, we lack an understanding on how their relative contribution varies along the fluvial continuum. In this thesis, I first review the spatial and temporal patterns of the controls leading to CO_2 supersaturation in fluvial systems. I then explicitly attempted to quantify all the major pathways involved in the fluvial CO_2 budget along the fluvial continuum in a boreal river network spanning Strahler river order 2 to 5. The resulting fluxes were then integrated within a mass balance framework, in order to test the combinations that best match the observed patterns in riverine pCO_2 along the fluvial network. This approach allows to account for uncertainties in the various pathways and to infer how their potential contribution to the stream CO_2 budgets may shift along the fluvial continuum. The downstream decline in the contribution of lateral groundwater inputs relative to total stream discharge was mainly responsible of its spatial decline in pCO_2 along the stream-river continuum. Internal metabolism, which averaged 0.81 g C m^{-2} d^{-1} and did not vary significantly downstream, became an increasing contributor to stream CO_2 fluxes downstream, as the contribution of lateral inputs declined. This study reinforces the need to combine multiple approaches to obtain an integrative perspective of riverine CO_2 dynamics. Understanding all of the major processes underlying stream CO_2 emissions is key to our understanding of this landscape feature, and for the prediction and extrapolation (spatial and temporal) at larger scale of lotic CO_2 emissions.

Keywords: *decline, continuum, metabolism, lateral inputs, gas transfer coefficient*

INTRODUCTION

Les systèmes aquatiques d'eau douce ne constituent qu'une infime proportion de la surface terrestre, mais représentent toutefois une composante importante du cycle global du C. Leurs rôles à la fois de transporteur, décomposeur et émetteur de C dans l'environnement font des systèmes aquatiques, des zones d'échange majeures entre les différents réservoirs : terrestre, océanique et atmosphérique. Il reste pourtant des lacunes dans nos connaissances quant aux processus déterminant ces échanges et leur régulation.

Le biome boréal est particulièrement pertinent dans l'étude du cycle du C puisqu'il détient près de 60 % du carbone organique (WBGU, 1998, Gorham et *al.,* 1991) et environ 471 Pg de C organique et inorganique dans ses sols (Dixon, 1994, Gorham et *al.,* 1991). L'eau drainant les sols se charge alors du C sous forme organique et inorganique (CO_2, CH_4, HCO_3^-) pour ensuite entrer dans les systèmes aquatiques. Actuellement, le flux global d'export de C (organique et inorganique) terrestre vers les écosystèmes aquatiques (rivières, lacs et réservoirs) est estimé entre 1.9 Pg C yr^{-1} et 5.1 Pg C yr^{-1} (Drake et *al.,* 2018, Regnier et *al.,* 2013, Aufdenkampe et *al.,* 2011, Cole et *al.,* 2007), soit environ 12 - 34 % du C fixé par l'écosystème terrestre (Butman et *al.,* 2016, Wallin et *al.,* 2013, Striegl et *al.,* 2012). Au cours de la dernière décennie, les estimations de l'export de C des sols vers les systèmes aquatiques n'ont eu de cesse d'augmenter, jusqu'à atteindre presque 5 fois la valeur donnée par Cole et *al.,* en 2007, soit 2.1 Pg C yr^{-1} (Drake et *al.,* 2018). Un effort croissant de la recherche de ces dernières années a visé à augmenter la précision ainsi que la qualité de ces apports terrestres (CO_2, carbone organique dissous ou DOC) aujourd'hui considérés comme

d'importants contributeurs à la sursaturation des milieux aquatiques en CO_2 (Leith et *al.,* 2015).

Le rôle des rivières autrefois considérés comme un conduit passif transportant le C des écosystèmes terrestres vers l'océan (Cole et *al.,* 2007, IPCC, 2013, Battin et *al.,* 2009, Aufdenkampe et *al.,* 2011), se révèle aussi comme un élément actif du cycle du carbone traitant et transformant une grande quantité du carbone terrestre transporté. De fait, parmi les 5.1 Pg yr^{-1} de carbone transporté par les eaux continentales, moins de la moitié atteindra l'océan (Drake et *al.,* 2018, Aufdenkampe et *al.,* 2011). Alors qu'une petite fraction (c.a. 22 %) est stockée dans les sédiments, la majeure partie est exportée vers l'atmosphère sous forme de CO_2 (Cole et *al.,* 2007, Aufdenkampe et *al.,* 2011). La sursaturation des rivières en CO_2 est donc le résultat à la fois d'apports terrestres en CO_2 biogéniques (eaux souterraines) et du métabolisme aquatique *in situ* (au sein de la colonne d'eau et des sédiments) du carbone organique terrestre (Demars 2019, Aufdenkampe et *al.,* 2011, Battin et *al.,* 2008). Bien que les apports latéraux soient souvent rapportés comme prédominants (Crawford et *al.,* 2014, Leith et *al.,* 2015, Winterdahl et *al.,* 2016, Deirmendjian and Abril, 2018, Magin et *al.,* 2017) en lien avec leur étroite connexion avec les sols, peu d'études ont tenté d'évaluer les contributions relatives de chacune de ces sources (Hotchkiss et *al.,* 2015, Lupon et *al.,* 2019).

Cependant, la contribution relative de chacun de ces processus varie de manière spatiale, en fonction de la taille des cours d'eau et des rivières par exemple (Hotchkiss et *al.,* 2015) ainsi que temporellement, notamment en lien avec l'hydrologie (Oviedo-Vargas et *al.,* 2015). La complexité de ces processus et de leurs interactions rend la quantification des sources relatives de CO_2 lotique difficile. Bien qu'un nombre important de publications aient pour objet l'étude du budget carbone des systèmes lotiques, elles résultent principalement de bases de données spatiales et temporelles fragmentées, affaiblies par leur manque de distribution spatiale ce qui les rendraient

potentiellement biaisées voire incorrectes. En dépit des récentes avancées de notre compréhension au regard du fonctionnement des systèmes aquatiques, de nombreuses incertitudes liées à l'estimation du rôle des facteurs modulant ces processus métaboliques et physiques à diverses échelles restent présentes. Connaître l'influence de ces processus sur la sursaturation en CO_2 dans les écosystèmes naturels à l'échelle d'un bassin versant est donc essentiel pour établir un budget carbone à l'échelle globale de façon plus précise et de meilleure qualité.

Le but de ce mémoire est d'une part de réaliser une revue littéraire concernant la contribution des entrées d'eaux souterraines et celle du métabolisme *in situ* dans le maintien de la sursaturation des rivières en CO_2 ainsi que d'élucider l'importance relative des contrôles et de leur variation sur la dynamique spatiale du CO_2 le long d'un continuum fluvial. En bref, je tenterai d'explorer à la fois le caractère d'émetteur de gaz des rivières ainsi que celui moins connu de réacteur de matière organique. Cette étude sera menée sur un réseau fluvial complet, en commençant par les cours d'eau les plus petits (ordre Strahler 1) et s'étendant ensuite jusqu'à des rivières d'ordre 5, dans la région boréale de La Côte Nord (Québec, Canada). Quatre campagnes d'échantillonnage ont été menées dans le but de capturer deux régimes hydrologiques distincts; un débit élevé résultant de la fonte des neiges du printemps et un débit de base faible typique de la saison estivale. Les objectifs de cette étude seront les suivants : **1)** examen de la littérature actuelle sur l'identification et la quantification des sources de C menant à la sursaturation des milieux lotiques en CO_2, **2)** comprendre la dynamique spatiale en pCO_2 observée dans les réseaux fluviaux, des petites rivières sources vers les rivières de plus gros calibres, en identifiant et quantifiant la contribution de chacun des contrôles impliqués.

CHAPITRE I

REVUE DE LITTÉRATURE SUR L'IDENTIFICATION ET LA QUANTIFICATION DES SOURCES ET PROCESSUS MENANT À LA SURSATURATION DES RIVIÈRES EN CO_2

Les rivières des régions boréales sont pour la plupart sursaturées en CO_2 vis à vis de l'atmosphère (*e.g.* Striegl et *al.,* 2012, Wallin et *al.,* 2010, Raymond et *al.,* 2013). Identifier et caractériser les contrôles majeurs menant à la sursaturation en C des rivières est le premier objectif de mon étude.

1.1 Processus à l'origine de la sursaturation des milieux lotiques en CO_2

1.1.1 Sources de CO_2

Les principaux processus contribuant à l'enrichissement en CO_2 des eaux de rivières sont: **(1)** les apports directs de CO_2 du sol, **(2)** la production de CO_2 *in situ* à partir de carbones allochtone et autochtone, ainsi que la dissolution de carbonates et la dégradation des minéraux silicatés.

(1) Les apports externes au cours d'eau peuvent être définis comme les flux entrants d'eau terrestre, d'écoulements de surface ou d'eaux souterraines profondes, qui transportent plusieurs espèces de C d'origine terrestre, notamment le CO_2, le CH_4 et le DOC (Fig. 1.4). Les écosystèmes terrestres présentent un stock important de carbone organique stocké dans les couches superficielles du sol, et ce, particulièrement au sein du biome boréal. Ce carbone subit d'importantes transformations lors de son transport via les eaux souterraines et les eaux du sol, avant d'être finalement chassé vers les eaux de rivière sous deux formes principales (Palmer et *al.*, 2001, Teodoru et *al.*, 2009): (a) **carbone inorganique** (CO_2, HCO_3^-) produit dans les sols par la respiration dans le cas de la production de CO_2 et par l'érosion dans le cas du HCO_3^- (Algesten et *al.*, 2004). (b) **Le carbone organique dissous** allochtone provient de la décomposition partielle de la matière organique dans les horizons superficiels du sol. Mobilisé, il est ensuite transporté vers les cours d'eau par le biais d'un écoulement latéral.

(2) Les processus *in situ* sont définis comme la formation ou la dégradation de CO_2 se produisant au sein du cours d'eau (Fig.1.2). Les processus internes générant du CO_2 comprennent la **minéralisation** (benthique et pélagique) du carbone organique, la **photo-oxydation du carbone organique**, la **précipitation des carbonates** et **l'oxydation du méthane** (Paerl et Pinckney, 1996). La production et la consommation de dioxyde de carbone dans les sols et les cours d'eau sont toutes deux influencées par la qualité et la quantité de matière organique, la disponibilité des éléments nutritifs, la température et l'apport en oxygène (*e.g.* Jones et Mulholland, 1998). La dissolution des carbonates (Geldern et *al.*, 2015) et l'altération des minéraux silicatés (Humborg et *al.*, 2011) dans les sols et les sous-sols sont d'autres processus susceptibles de générer des composés inorganiques du carbone (HCO_3^-) dans les cours d'eau. Étant donné que cette étude a lieu à La Côte Nord au Québec, où prédomine le bouclier précambrien (roches granitiques), les processus impliquant les carbonates sont généralement négligés. Pourtant de récentes études soulignent l'importance de la dégradation des silicates dans

ce type de paysages (Berner and Berner, 2012, Marx et *al.*, 2017). Dans des eaux à pH inférieur à 6, le CO_2 est la forme de carbone inorganique dissous (DIC) la plus abondante. Il contribue alors à l'altération des minéraux silicatés, une réaction qui libère des ions bicarbonates (HCO_3^-). À un pH compris entre 6 et 8, HCO_3^- est l'espèce prédominante et représenterait plus de 50% du pool de DIC. Dans ces cas, la DIC ne doit pas être utilisée comme un proxy du CO_2 et inversement.

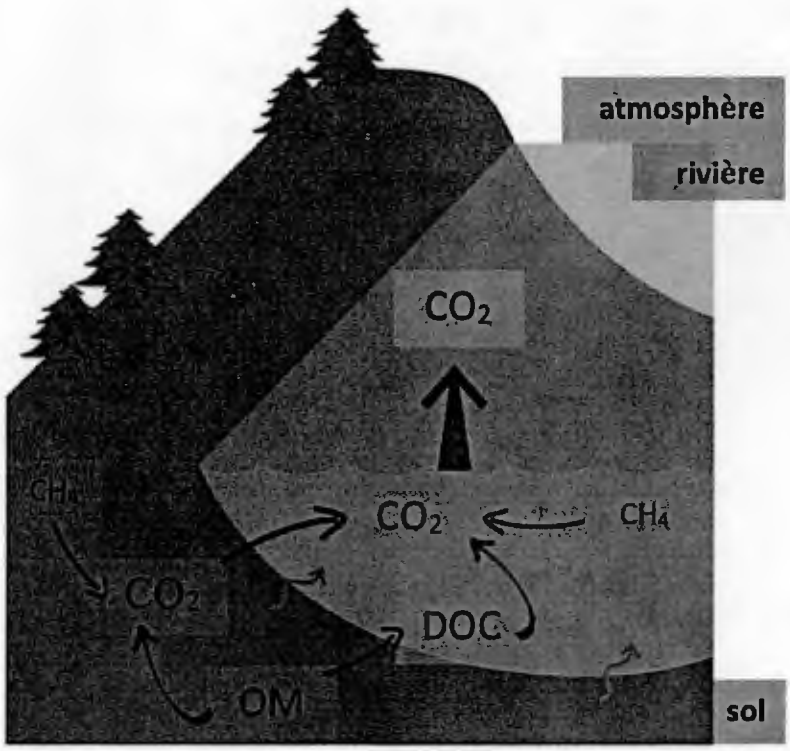

Figure 1.1 Sources et processus menant à l'émission de CO_2 des rivières : (1) minéralisation de la matière organique terrestre (OM) et transfert du CO_2 des sols vers la colonne d'eau, (2) minéralisation des matières organiques dissoute (DOC) et particulaire autochtone au sein de la colonne d'eau, (3) oxydation du CH_4 terrestre puis transfert vers la colonne d'eau et oxydation du CH_4 autochtone au sein de la colonne d'eau. ***N.B. Les processus considérés comme mineurs dans cette étude ne sont pas représentés, i.e. la dissolution et l'altération des carbonates, ainsi que la photodégradation.***

1.1.2 Processus physiques influençant la sursaturation en CO_2

Outre la contribution relative des différentes sources de CO_2, certains processus physiques liés au bassin versant ou à la colonne d'eau, sont d'autres facteurs clés liés à l'état de supersaturation d'un cours d'eau. Il est important de les comprendre pour pouvoir quantifier le CO_2 perdu vers l'atmosphère au sein d'un réseau hydrographique. Un outil communément utilisé par les limnologues, particulièrement en milieu lentique, est le coefficient de transfert gazeux *k,* il décrit l'échange d'un gaz à l'interface eau-air. Ce processus est entre autres, contrôlé par la turbulence de l'eau (Macintyre et *al.,* 1995), laquelle dépend à son tour de la vitesse du courant, des forces de frottement au niveau du lit du canal ainsi que de la vitesse du vent (*e.g.* Beaulieu et *al.,* 2012). En connaissant les sources et les processus contrôlant les émissions de CO_2 dans les cours d'eau, il est alors possible d'en explorer les variations spatiales à travers un continuum fluvial.

1.2 Émissions de CO_2

Comme la plupart des cours dans le monde sont sursaturés en CO_2 par rapport à l'atmosphère sus-jacente, ils agissent comme des sources de carbone pour l'atmosphère (Hope et *al.,* 1994, Humborg et *al.,* 2010, Aufdenkampe et *al.,* 2011, Butman et Raymond, 2011, Crawford et *al.,* 2013, Borges et *al.,* 2015). Les études faisant l'estimation de l'évasion lotique de CO_2 depuis la surface de l'eau révèlent une variabilité considérable d'un paysage à un autre, à l'échelle régionale ou continentale (Aufdenkampe et *al.,* 2011, Butman et Raymond, 2011) ou même au sein même d'un bassin versant (Alin et *al.,* 2011, Campeau et *al.,* 2014). Ces tendances observées s'expliquent par la variation des facteurs géographiques, des propriétés physiques du réseau hydrographique (couverture terrestre, métabolisme terrestre) ainsi que de la

colonne d'eau elle-même, telle que la connectivité à l'interface eau-sol et la production *in situ* (Alin et *al.,* 2011).

Malgré leur faible couverture géographique, les rivières de tête constituent le « réseau capillaire » du bassin versant, comme Wallin et *al.,* (2013) les décrits; une zone d'échange clé entre les systèmes terrestre et aquatique. Un grand nombre d'études soulignent la contribution majeure des ruisseaux dans l'émission de CO_2 (les plus récentes : *e.g.* Lupon et *al.,* 2019, Marx et *al.,* 2017, Rasilo et *al.,* 2017). Leur étroite connexion avec le réseau terrestre adjacent est souvent rapportée comme étant l'une des causes principales de la sursaturation des petites rivières (Strahler order < 3). Une perte de CO_2 s'effectue ensuite vers les rivières de plus grand calibre, où un déclin progressif de la concentration et des émissions de gaz est observé le long de réseaux fluviaux (*e.g.* Teodoru et *al.,* 2009, Wallin et *al.,* 2010, Campeau et *al.,* 2014, Hotchkiss et *al.,* 2015). Cette tendance s'explique généralement par une combinaison de facteurs impliquant un changement des sources de CO_2 (Butman et Raymond, 2011, Humborg et *al.,* 2010, Wallin et *al.,* 2010, Teodoru et *al.,* 2009) et d'autres processus physiques liés aux caractéristiques du réseau hydrographique (*e.g.* connectivité au milieu terrestre, turbulence de l'eau, pente, géologie), ainsi qu'à la vitesse du vent (Jones et Mulholland, 1998). De plus, les rivières de tête démontrent une plus grande variabilité de concentrations et d'émissions de CO_2 en comparaison aux rivières d'ordre plus important, ce qui reflète donc l'hétérogénéité et la réactivité importantes de ces systèmes (Teodoru et *al.,* 2009, Campeau et *al.,* 2014). Afin de mieux comprendre la dynamique des émissions de CO_2 au sein d'un réseau hydrographique, il est crucial de mesurer l'importance relative de chacune des différentes sources et processus à l'origine de la sursaturation en CO_2 dans les cours d'eau.

1.3 Variabilité spatiale dans les sources et les processus à l'origine des concentrations et des flux de CO_2 des cours d'eau

Comme indiqué dans le paragraphe précédent, parmi les processus pouvant conduire à une sursaturation en CO_2 des cours d'eau, les apports terrestres sont majoritairement rapportés comme l'un des facteurs majeurs (Crawford et *al.,* 2014, Leith et *al.,* 2015, Winterdahl et *al.,* 2016, Deirmendjian and Abril, 2018, Magin et*al.,* 2017). Pourtant, la contribution relative de l'apport direct de CO_2 terrestre par rapport à la production interne de CO_2 à la rivière au sein d'un réseau hydrographique n'est pas bien documentée (Hotchkiss et *al.,* 2015). Toutefois, des études composées de données spatiales fragmentées suggèrent une source terrestre dans les rivières de tête, en raison de leur couplage étroit avec l'écosystème terrestre environnant (Hopeet *al.,* 2004, Humborg et *al.,* 2010, Crawford et *al.,* 2013, Campeau et *al.,* 2014, Hotchkiss et *al.,* 2015). Par exemple, Hotchkiss et *al.,* (2015) ont estimé que les intrants de CO_2 terrestres seraient à eux seuls responsables de 86 % des flux de CO_2 dans les ruisseaux (Strahler order faible). Des apports terrestres élevés (Humborg e t*al.,* 2010) couplés à des processus physiques liés à la topographie du bassin versant (Duvert et *al.,* 2018, Smits et *al.,* 2017), comme les pentes abruptes qui, générant de la turbulence (Alin et *al.,* 2011), expliqueraient les fortes émissions de gaz en amont.

Lorsque l'on se déplace vers l'aval, bien que les apports terrestres constitueraient toujours la principale source d'émissions de CO_2, le CO_2 dérivé du sol diminuerait proportionnellement à l'augmentation du volume d'eau. Hope et *al.,* en 2002 ont montré que la diminution de la connectivité avec le milieu terrestre, serait responsable du déclin des émissions de CO_2 des petits vers les grands cours d'eau. En parallèle, plusieurs études reportent une importante contribution du métabolisme interne à la rivière comme source de CO_2, dans la zone hyporhéique notamment (Boodoo et *al.,* 2017, Rasilo et *al.,* 2017). Hotchkiss et *al.,* 2015 suggèrent que la production de CO_2

in situ est responsable à son tour d'une proportion plus élevée d'émissions de CO_2 dans les rivières de plus gros calibre (temps de résidence plus élevé), mais montrent toutefois une tendance au déclin à l'échelle du bassin versant. Par ailleurs, d'autres études suggèrent que le DOC d'origine terrestre pénétrant dans les eaux de tête est probablement plus labile et donc plus sujet à la dégradation microbienne que le DOC en aval, plus récalcitrant à la biodégradation (Berggren and del Giorgio, 2015). De plus, alors que les petits cours d'eau sont des points chauds pour l'évasion de gaz, les plus grands cours d'eau et les rivières émettent moins de C dans l'atmosphère, mais constituent de vastes zones de haut débit dégagées et donc plus exposées au vent (Marx et *al.,* 2017).

Les tendances rapportées ci-dessus présentent un aperçu des tendances auxquelles je pourrais m'attendre dans mon étude. Pourtant, ces observations restent conceptuelles, et reposent sur des calculs via des modèles ou des déductions (Hope et *al.,* 2004, Hotchkiss et *al.,* 2015). L'identification des sources d'émissions de CO_2 et des mécanismes qui les contrôlent tout au long d'un réseau de cours d'eau a rarement été réalisée, en particulier à l'échelle du bassin versant (Lupon et *al.,* 2019). Il est nécessaire de quantifier les processus clés dans le cycle biogéochimique des rivières, et ce, intégré au sein d'un réseau fluvial afin de caractériser l'influence relative de chacun sur les budgets C des milieux lotiques.

1.4 Variabilité temporelle des sources et processus à l'origine des concentrations et des flux de CO_2 dans les cours d'eau

L'hétérogénéité des concentrations de CO_2 le long du réseau hydrographique a également un aspect temporel. La variabilité saisonnière dans les systèmes fluviaux a été principalement associée à l'hydrologie (Laudon et *al.,* 2007, Ågren et *al.,* 2007, Lynch et *al.,* 2010) et à l'activité biologique (Lynch et *al.,* 2010). L'alternance des

saisons hydrologiques affecte généralement les voies d'écoulement préférentiel du sol vers les rivières et ce, jusqu'à en modifier la dynamique du C dans le cours d'eau adjacent. Une année hydrologique peut être divisée en 3 périodes distinctes caractérisées par: **(1)** un couvert nival, **(2)** la fonte des neiges et **(3)** libre des glaces (Ågren et *al.,* 2007).

(1) Pendant la **saison hivernale**, le cours d'eau est à un débit de base et n'est alimenté que par des eaux souterraines profondes. Le sol gelé recouvert de neige limite les flux de carbone environnants et l'eau reste donc pauvre en carbone (Lynch et *al.,* 2010). Entre temps, alors que l'eau froide ralentit la décomposition microbienne, la lumière parvient toujours à pénétrer dans la colonne d'eau, soutenant ainsi la production primaire. Cette saison ne sera pas le sujet de cette étude.

(2) Le **printemps** est considéré comme un événement hydrologique majeur de l'année dans les paysages boréaux, exportant en moyenne 47 % du carbone organique dissous (DOC) allochtone aux systèmes aquatiques adjacents (Ågren et *al.,* 2010). Bien que la dynamique du DOC soit relativement cohérente d'une étude à l'autre, celle du CO_2 reste variable. Campeau et *al.,* en 2014 observent la contribution de la fonte printanière aux émissions annuelles de CO_2, suggérant un rôle important de l'hydrologie dans le contrôle des concentrations et des émissions de CO_2 dans le cours d'eau. Au contraire, Doctor et *al.,* en 2008 ont révélé que la concentration de carbone inorganique dissous (DIC) dans les cours d'eau était faible pendant la fonte des neiges, ce qui suggère que les processus biologiques contrôlant les concentrations de CO_2 via la dégradation du carbone organique sont ralentis pendant la saison la plus froide. Une autre étude rapporte également une diminution des concentrations de DIC et pourrait être la conséquence d'un phénomène de dilution (thèse « Géochimie et flux de carbone organique et inorganique dans les milieux aquatiques de l'est du Canada: exemples du Saint-Laurent et du réservoir Robert-Bourassa: approche isotopique », Hélie, 2004).

(3) La **saison sans couvert de neige** (5-6 mois) est constituée d'une alternance de périodes sèches et humides. Environ 40 % du DOC annuel peut être exporté vers les cours d'eau, essentiellement lors de précipitations (Ågren et *al.,* 2007). Lynch et *al.,* en 2010 suggèrent des taux de respiration plus élevés dans le sol et dans l'eau entre mai et juillet, caractérisés par des débits, des températures et des émissions de gaz élevés (Campeau et *al.,* 2014). Lors des événements de précipitation, la DOC et la DIC précédemment produits et stockés pendant les périodes sèches dans les sols (Freeman et *al.,* 2002, Doctor et *al.,* 2008) sont remobilisés et transportés vers les cours d'eau.

Les deux saisons les plus importantes du biome boréal pour les systèmes lotiques sont donc : la saison de la fonte des neiges et la saison sans neige, donnant une image d'un système à débit élevé se produisant juste après la fonte des neiges (cours d'eau à son débit le plus élevé) et d'un système à bas débit en été (cours d'eau alimenté uniquement par les eaux souterraines).

Ces tendances saisonnières ajoutent une complexité quant à la caractérisation des sources et des processus susceptibles d'influencer les concentrations et les émissions de C dans les systèmes fluviaux. Les informations présentées ci-dessus sont tirées de publications basées sur des sites spécifiques, et de courtes périodes de temps. Seules quelques études dans les bassins versants traitant de la variabilité temporelle des différentes sources de CO_2 le long d'un réseau hydrographique existent dans la littérature. Ceci limite donc grandement notre capacité à construire des budgets de carbone des rivières.

1.5 Objectifs et hypothèses

Bien que de nombreuses études reportent aujourd'hui un déclin des pressions partielles en CO_2 (pCO_2, µatm) des rivières sources vers les rivières de plus gros calibres (*e.g.*

Campeau et *al.*, 2014, Hotchkiss et *al.*, 2015, Teodoru et *al.*, 2009, Crawford et *al.*, 2013) comme observé en Figure 1.2, les facteurs responsables de ce patron aujourd'hui bien connus, restent mal quantifiés. Les caractériser et mesurer leurs impacts sur la dynamique du C fluvial constitueront les objectifs de mon second chapitre.

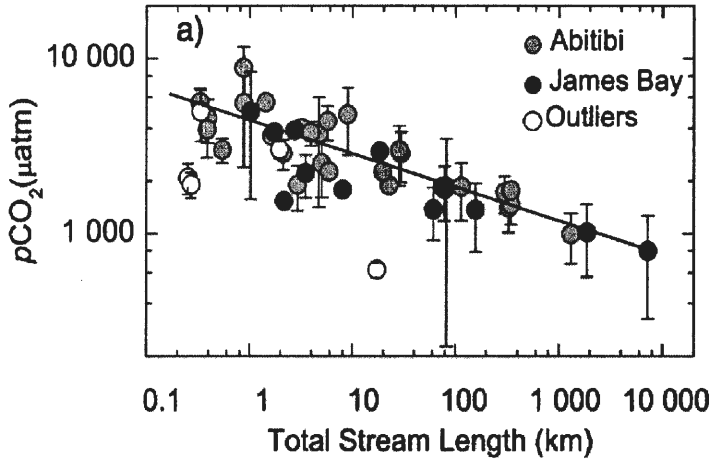

Figure 1.2 Graphique représentant les variations spatiales (gauche vers la droite = de la source vers les rivières plus larges) des pressions partielles en CO_2 (en µatm) de rivières localisées dans plusieurs régions du Québec. Chaque point est la moyenne des valeurs de pCO_2 de sites de chacune des régions étudiées. *Source : Campeau* et *al., 2014*

A l'aide des données récoltées dans le bassin versant de *La Petite Romaine*, Québec, Canada, j'examinerai la distribution du pCO_2 tout au long du continuum fluvial et m'attendrai à y voir un déclin des concentrations, comme précédemment observé dans la littérature (Fig. 1.2, Campeau et *al.*, 2014), des rivières sources vers les plus larges. Il est à noter, que bien que leurs concentrations en C soit attendues à diminuer au sein du réseau hydrographique, je prévois néanmoins que les rivières présenteront une sursaturation constante en CO_2. Parmi les facteurs identifiés comme étant importants dans le contrôle de la dynamique du C de ces réseaux, j'étudierai en particulier : **1)** les apports latéraux transportant à la fois l'eau souterraine, ainsi que du carbone organique et inorganique en provenance des sols, **2)** les concentrations en CO_2 et DOC des sols à

proximité des rivières étudiées, **3)** le métabolisme interne à la rivière, résultat de la balance entre production primaire (GPP, dégradation de CO_2) et respiration (ER, production de CO_2) et **4)** le processus d'échange gazeux (k) entre la surface de la colonne d'eau et l'atmosphère ayant un rôle crucial dans les flux d'émissions. Il est donc attendu que l'au moins un de ces contrôles varie au long du réseau fluvial pour expliquer ce déclin en CO_2 au sein du réseau hydrographique (hypothèses illustrées dans la figure 1.3):

(1) Un déclin de l'apport en C de l'eau souterraine

(2) Une diminution des concentrations en CO_2 et DOC des sols alimentant les rivières à proximité

(3) Une diminution du métabolisme *in-situ* à mesure que les rivières s'élargissent

(4) L'augmentation du coefficient d'échange gazeux (k) des petites vers les rivières de plus gros calibres, générant ainsi plus d'émissions gazeuses, contribuant à la perte de CO_2 fluvial (Fig. 1.2).

L'apport des sources contribuant à la sursaturation du CO_2 des rivières se voyant diminuer et le processus d'échange gazeux vers l'atmosphère augmentant, la variation de ces deux facteurs (amplitude et patron) serait donc responsable du déclin observé en CO_2 au sein d'un continuum fluvial.

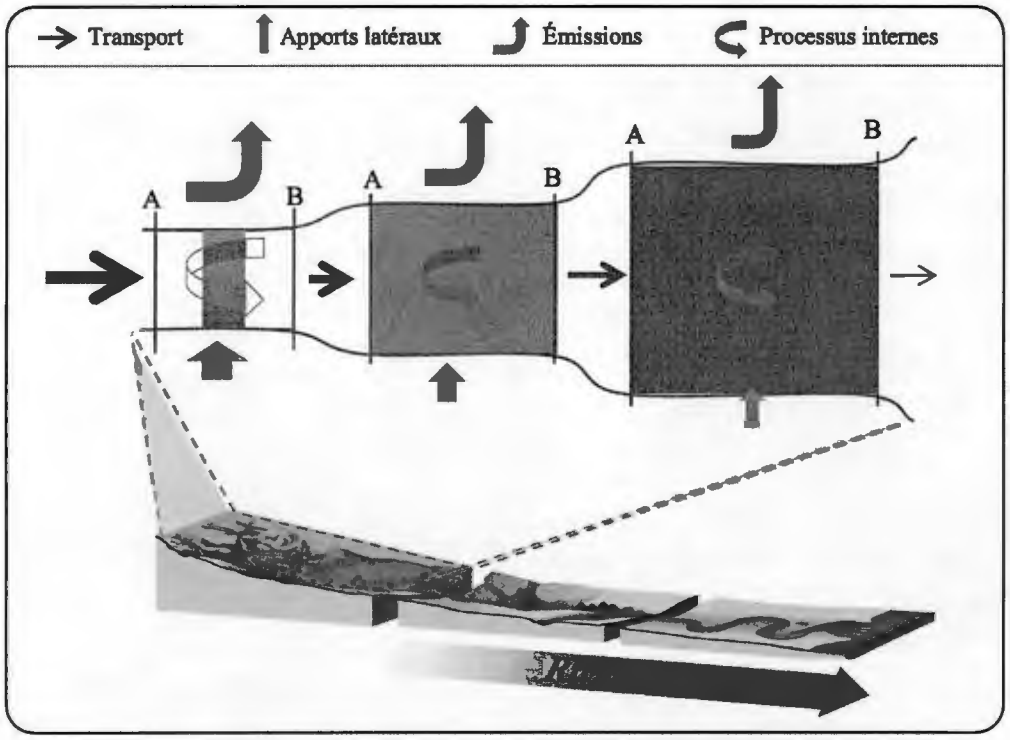

Figure 1.3 Schéma représentant la variation attendue des divers flux (d'apports ou de pertes de CO_2) impliqués dans la sursaturation et la diminution en CO_2 des rivières au sein d'un réseau hydrographique. Ce réseau, aussi appelé « continuum fluvial », est découpé en tronçon représentant chacun une section de la rivière de l'amont A) vers l'aval B). Nous avons réalisé un bilan de masse dans chacune de ces sections (seulement 3 représentés ici). Les flux de C considérés sont : l'évasion des gaz à l'interface eau-air, les processus métaboliques internes et les apports latéraux des eaux du sol vers la rivière.

Une fois ces hypothèses comparées aux données mesurées, il s'agira alors d'intégrer les tendances et magnitudes observées de chacune des variables considérées, dans un bilan de masse, dans le but de recréer la tendance spatiale de pCO_2 observée (mesurée) dans les rivières. Dans le cas où la pCO_2 recréée est similaire à celle observée, alors nos estimations et les méthodes utilisées sont donc jugées acceptables ou leurs erreurs se compensent de façon à recréer des flux justes. Enfin, nous testerons si la solution de chacun des bilans de masse appliqué à chaque segment est variable tout au long du continuum fluvial.

1.6 Approche utilisée

Notre approche consiste tout d'abord à quantifier les principaux processus intervenant dans la détermination de la pCO_2 dans les cours d'eau et à évaluer leur variation spatiale, *i.e.* des ruisseaux de tête de bassin vers les rivières de calibre plus important (continuum fluvial). Nous intégrons ensuite ces processus au sein d'un bilan de masse, dans le but d'évaluer la combinaison de facteurs sélectionnés. Pour ce faire, le réseau fluvial de La Petite Romaine est découpé en tronçons de *Strahler order* croissant, chacun délimité par un site A en amont, s'écoulant vers un site B, à l'aval. Pour chacun de ces tronçons, la balance des flux de CO_2 est donc représentée par la somme de tous les processus intervenant dans le tronçon de rivière, y compris le flux entrant en amont (A) (f_R), les apports latéraux (f_s), les pertes par émissions vers l'atmosphère (f_e) et les processus internes au segment (*e.g.* métabolisme), qui équivaut aux flux sortants à l'aval (B) (f_o). L'équation (1) du bilan massique peut donc s'exprimer comme suit:

$$f_o = f_R + f_s - f_e \pm f_m \qquad (1)$$

Tous les flux sont exprimés en g C m^{-2} d^{-1}, *i.e.* la masse de C par surface de rivière par jour.

Ce bilan de masse en CO_2 des rivières du réseau, comprend donc la géomorphométrie du chenal, les entrées latérales d'eau, le CO_2 et le DOC transportés par les eaux souterraines, le coefficient d'échange gazeux (contrôle clé de l'évasion) et le bilan métabolique *in situ*. En somme, cette étude examine le rôle potentiel que l'équilibre chimique de l'eau et la spéciation du C pourraient jouer dans la détermination du CO_2 lotique.

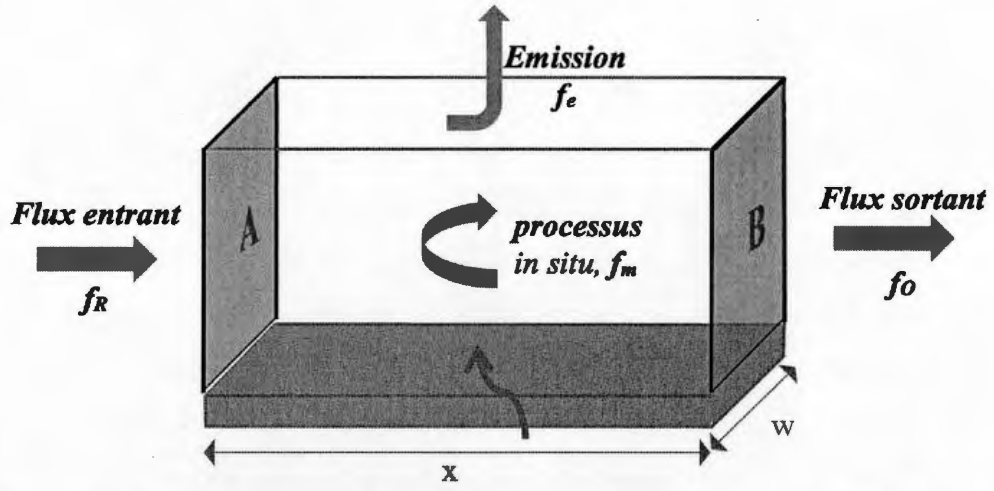

Figure 1.4 Représentation schématique d'un segment théorique de rivières, bordé des sections A (amont) et B (aval). Chacun des flux (*f*) sont représentés par des flèches, soit entrante dans le cas d'un flux positif, soit sortante dans le cas d'un flux négatif. Le rectangle transparent symbolise la colonne d'eau de la rivière, et le rectangle gris, la zone hyporhéique sous-jacente. Les lettres w et x, sont respectivement associées à la largeur et la longueur du segment de rivière.

Enfin, l'utilisation de multiples approches et techniques de mesures, nous donnera des perspectives différentes puisque souvent empruntées à des milieux différents, incluant la limnologie, l'hydrologie, et la pédologie. Ainsi, une approche plus intégrative et écosystémique sera privilégiée, considérant les mécanismes se produisant au sein de la rivière et à ses interfaces. Le cours d'eau constitué de la colonne d'eau et de la zone hyporhéique, sera placé au sein d'un système spatio-temporel, intégrant le milieu aquatique, les zones ripariennes l'entourant, le milieu hydrologique souterrain et le milieu atmosphérique sus-jacent.

CHAPITRE II

UNDERSTANDING THE PROCESSES UNDERLYING THE PATTERN OF pCO_2 DECLINE ALONG A RIVERINE CONTINUUM

2.1. Abstract

Stream ecosystems are a major source of CO_2 emissions to the atmosphere and contribute significantly to the global C budget. Whereas the main pathways underlying CO_2 dynamics in streams and rivers are generally known, their relative contributions and how these change along the fluvial continuum are still not well understood. Here, we measure the main pathways underlying the spatial pattern of pCO_2 along the fluvial continuum (order 1 to 5) in a boreal river network, for both the late spring and mid-summer periods. We have quantified ambient stream discharge and CO_2 concentrations, lateral inputs of CO_2 and DOC, in-stream CO_2 production, and gas evasion and have integrated these components within a mass balance framework. Our results show that the stream pCO_2 declined along the continuum both in spring and summer, from an average of 2 398 ± 537 µatm SD in the headwater streams to 687 ± 138 µatm SD downstream, whereas emissions declined from 4.71 ± 4.77 g C m^{-2} d^{-1} in the 1st segment to 0.79 ± 0.40 g C m^{-2} d^{-1} downstream in the river. Lateral inputs of soil-derived CO_2 were a large contributor to stream CO_2 supersaturation and emissions

in the headwaters (median = 76 %), and the downstream decline in pCO_2 was mainly due to a decline in the contribution of lateral water inputs relative to total stream discharge along the stream-river continuum. The rate of in-stream CO_2 production derived both from differences in DOC concentration between soil and stream waters, and from diel O_2 metabolism estimates, converged to median values of 0.81 g C m^{-2} d^{-1}, along the entire continuum. Internal metabolism contributed on average 24 % of the total estimated stream CO_2 fluxes, but this contribution greatly increased downstream, reaching 40% in order 5 rivers. Internal production of CO_2 appears to be critical in determining the position of the plateau of supersaturation that will be attained at the higher stream orders within the network. Overall, our results clearly suggest that whereas external inputs explain CO_2 dynamics at the headwaters, it is the combination of external and internal inputs together that explained both CO_2 outgassing and the ambient levels of CO_2 at the whole network scale, highlighting the need for integrative studies of riverine CO_2 dynamics that include all of the major processes underlying stream CO_2 emissions.

2.2. Introduction

Stream ecosystems are generally supersaturated in CO_2 and act as major emitters of CO_2 to the atmosphere (Humborg et *al.*, 2010, Aufdenkampe et *al.*, 2011, Butman and Raymond, 2011, Crawford et *al.*, 2013, Wallin et *al.*, 2013), contributing significantly to the global C budget (Raymond et *al.*, 2013). The degree of riverine CO_2 supersaturation varies widely both temporally and spatially (*e.g.* Hutchins et *al.*,2019, Lupon et *al.*, 2019, Duvert et *al.*, 2018, Marx et *al.*, 2017, Rasilo et *al.*, 2017, Campeau & del Giorgio, 2014). The large variability in fluvial CO_2 reflects the complexity of the biogeochemical functioning of rivers, as well as the complexity of their interactions with the surrounding watersheds (Wallin et *al.*, 2010). The degree of supersaturation within a fluvial network results from the combination of the injection of terrestrially-

derived CO_2, the internal production of CO_2 and the loss of CO_2 to the atmosphere (Lupon et *al.*, 2019, Duvert et *al.*, 2018, Liu et *al.*, 2018, Marx et *al.*, 2017, Rasilo et *al.*, 2017, Hotchkiss et *al.*, 2015, Leith et *al.*, 2015, Öquist et *al.*, 2009, Lyon et *al.*, 2010, Humborg et *al.*, 2010). In some watersheds, chemical processes may further influence the CO_2 balance (Campeau et *al.*, 2018, Marx et *al.*, 2017). The reported contribution of these processes varies within the literature: some studies point to terrestrial-derived CO_2 as the dominant pathway (Duvert et *al.*, 2018, Crawford et *al.*, 2014, Leith et *al.*, 2015, Winterdahl et *al.*, 2016, Deirmendjian and Abril, 2018, Magin et *al.*, 2017), whereas other studies have highlighted the role of internal CO_2 production as a major pathway fueling fluvial CO_2 (Rasilo et *al.*, 2017, Hotchkiss et *al.*, 2015, Peter et *al.*, 2014). It is clear that the relative contribution of these pathways to riverine CO_2 dynamics is extremely variable, and there is still discussion as to when and where one dominates over the other (Duvert et *al.*, 2018, Marx et *al.*, 2017, Hotchkiss et *al.*, 2015).

One of the most recurrent patterns in riverine CO_2 dynamics is a systematic decline of concentration as a function of river order along the fluvial continuum, which has been repeatedly observed across many different networks (Lupon et *al.*, 2019, Rasilo et *al.*, 2017, Hotchkiss et *al.*, 2015, Campeau et *al.*, 2014, Aufdenkampe et *al.*, 2011, Butman and Raymond, 2011, Wallin et *al.*, 2010, Humborg et *al.*, 2010, Teodoru et *al.*, 2009). This decline is most evident from very small headwater streams to medium sized rivers, since pCO_2 tends to stabilize at lower levels of supersaturation at higher order rivers (Hutchins et *al.*, 2019, Liu and Raymond, 2018, Teodoru et *al.*, 2009). Higher concentrations in headwater streams have been interpreted as reflecting a strong land-stream connectivity dominated by soil-derived CO_2 via lateral water inputs (Crawford et *al.*, 2014, Leith et *al.*, 2015, Deirmendjian and Abril, 2018). The subsequent declining trend in fluvial CO_2 downstream has been explained by a progressive loosening of this soil/stream linkage through a decline in the relative contribution of

lateral groundwater inputs (Duvert et *al.*, 2018, Leith et *al.*, 2015), and a concomitant increase in the relative contribution of internal pathways to CO_2 supersaturation (Rasilo et *al.*, 2017, Marx et *al.*, 2017, Hotchkiss et *al.*, 2015). There may also be systematic shifts in the intensity of the water/air gas exchange along the hydrologic continuum, driven by differences in average channel slope, water velocity and turbulence, which influence degassing and therefore may further modulate the downstream pattern in ambient pCO_2 (Raymond et *al.*, 2012, Öquist el *al.*, 2009, Wallin et *al.*, 2011).

Although this basic framework underlies the spatial pattern in pCO_2 within all fluvial networks, there is a wide variability in literature reports regarding the relative contribution of both soil-derived CO_2 and internal CO_2 production to fluvial CO_2 supersaturation along the fluvial continuum (Butman and Raymond, 2011, Hotchkiss et *al.*, 2013, Lupon et *al.*, 2019, Hope et *al.*, 2004, Johnson et *al.*, 2008). Part of the discrepancies may originate from the application of different approaches, or from addressing the issue at different portions of the network. There are major challenges associated to building stream CO_2 budgets necessary to quantify the relative contribution of external versus internal pathways, since each of the individual processes involved, *i.e.* soil water C inputs, *in situ* stream metabolism, CO_2 outgassing and particularly the gas exchange coefficient, is each associated with major methodological challenges. This explains the scarcity of studies that have quantified all these components. One of the most comprehensive studies to date, that of Lupon et *al.*, (2019) quantified the main components of CO_2 dynamics (except gas exchange, which was derived), by carrying out a full mass balance, and concluded that the CO_2 mass balance was essentially dominated by groundwater inputs. This study, however, was done along a stretch comprising a single stream order (order 1). Other studies have addressed the issue at larger scales spanning multiple river orders (Deirmendjian and Abril, 2018, Venkiteswaran et *al.*, 2014, Hotchkiss et *al.*, 2013, Crawford et *al.*, 2013, Butman and Raymond, 2011), but these studies have not actually quantified all the

main components of the mass balance, but rather addressed some elements and derived others by modeling or by difference.

It is clear that understanding the processes shaping the observed fluvial CO_2 dynamics and how these shift along the fluvial continuum requires an integrative approach that explicitly accounts for the main components of the C balance of these streams, simultaneously and at appropriate spatial and temporal scales, something that has rarely been attempted. Here we build the complete stream CO_2 balance at 4 segments along a fluvial continuum ranging from Strahler order 2 to 5 within a boreal watershed located in the la Cote Nord region of boreal Québec, Canada. We have carried out measurements of ambient stream discharge, CO_2, DOC concentrations, and water isotopes (^2H, ^{18}O) and combined these with estimates of external C inputs, using direct measurements of soil-water C concentrations, as well as direct estimates of air-water gas exchange using floating chambers. We further estimated ambient stream metabolism (respiration and gross primary production) using both continuous high frequency O_2 measurements and shifts in DOC concentrations. These factors were then integrated into a riverine CO_2 mass balance at the different segments along the fluvial network. This mass balance framework allowed us to explore how these different processes combine to yield the observed declining pattern in ambient stream pCO_2 along the fluvial continuum in this boreal watershed.

2.3. Material and methods

2.3.1. General approach: a quantitative framework

Our approach was to first quantify the major processes involved in determining ambient stream pCO_2 and to assess how these vary along the fluvial continuum, from headwater streams to larger order rivers. We then integrated these processes within a mass balance framework, with the objective to test if this combination of factors yielded realistic solutions. We then used the resulting mass balance solutions to assess how the relative contribution of the main processes influencing ambient stream pCO_2 varies along the fluvial continuum and seasonally in *La Petite Romaine* fluvial network. We defined 4 stream segments of increasing Strahler order that were free of tributary inputs, and mass balanced the CO_2 fluxes of each of these reaches. For each reach, the CO_2 export at the downstream end of the segment (f_o) should be equivalent to the upstream import of carbon (f_R) in addition to the major processes occurring within the reach, including the external input of CO_2 from soils (f_s), emissions of CO_2 to the atmosphere (f_e) and *in situ* net ecosystem metabolism (f_m). Therefore, the CO_2 mass balance for each segment can be expressed as follows:

$$f_o = f_R + f_s - f_e \pm f_m \quad (1)$$

2.3.2. Site information and context

We sampled 5 permanent streams (from Strahler order 1 to 5, Fig. 2.1, Supplementary Table B.3) in *La Petite Romaine* watershed in the boreal Côte-Nord region in Québec, Canada (50.3 – 51.4 °N and 63.9 – 63.2 °W) (Fig. 2.3). The Petite Romaine stream drains primarily acidic Spodosols (USDA classification), as well as some localized Histosols (USDA classification) immersed almost year-round at high elevation and low slope. Located on the Canadian Shield dominated by Precambrian rocks, surface waters

do not show evidence of carbonate formation (Schindler et *al.,* 2018; Soil Carbon Database, 1996) and are characterized by waters of low dissolved inorganic carbon concentrations and low alkalinity. Running waters have sandy to rocky bottoms, with humic colored waters and low turbidity. There were few macrophytes within river channels, but the banks were vegetated, mainly by *Alnus viridis* (Chaix) D.C., *Salix* spp., Poaceae spp., and mosses. The vegetation cover in the watershed mostly consists of stands of black spruce (*Picea mariana* (Mill.) B.S.P.) and balsam fir (*Abies balsamea* (L.) Mill) with some white birch (*Betula papyrifera* Marsh) and tamarack (*Larix laricina* (Du Roi) K. Koch). All sites were covered by grasslands, surrounded by taïga. The mean annual air temperature is 0.5 °C and the mean annual precipitation is 1 057 mm (from Havre St Pierre meteorological station, mean over a 30-year period, Environment of Canada), with elevations ranging from 496 to 837 m above sea level. The sampling campaigns were carried out in June and August of 2015 and 2016 to include data from two major hydrological periods characterizing northern landscapes, *i.e.* snowmelt high-flow conditions in June and base-flow conditions in August.

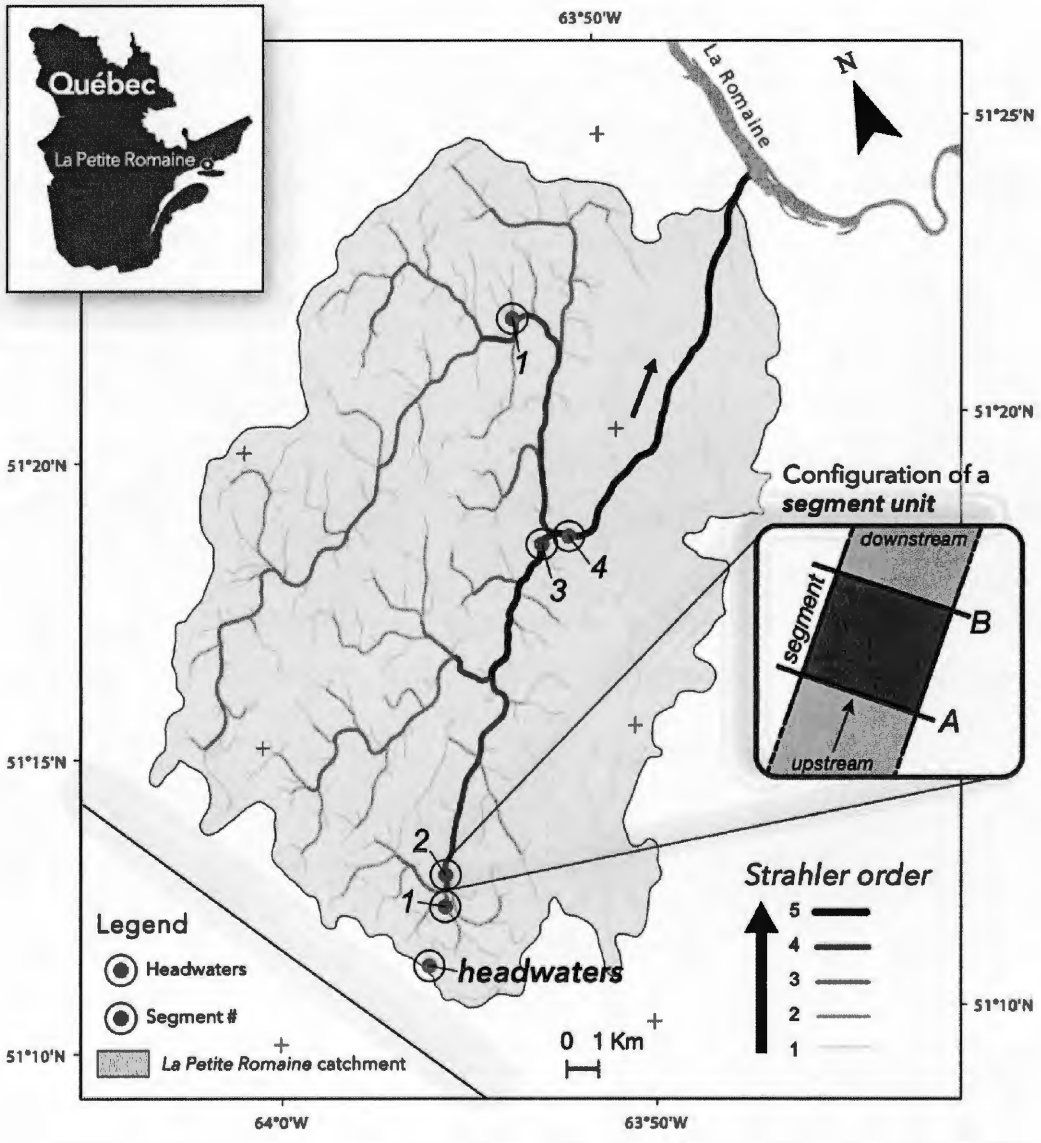

Figure 2.1 Location of *La Petite Romaine* stream network in la Côte Nord, Québec. The solid blue circle represents the headwaters site, not a segment on its own as it is only composed of a single site. The green solid circles appearing on the stream line, each represent a segment from 1 to 4, and from Strahler order 1 to 5. *Note that 2 green circles report number "1" on the map above: draining similar watershed areas, these 2 segments were averaged in order to constitute a single segment #1 used later on in this study.*

As an estimate of the downstream distance from the headwaters, we first determined the river length (flow length tool ArcGIS) based on a digital elevation model (23 m x 23 m) obtained via GeoBase resources, from which we derived the Strahler order of each stream. Strahler order 1 was arbitrarily given to an endmember stream at the top of the watershed. Within each stream, we sampled two points (top and the other downstream), delimiting a segment used in a mass balance perspective. Segments were selected on the basis of the following criteria: to cover a uniform stream order within each of the streams, their accessibility by helicopter and their homogeneity (*e.g.* no major rapids or tributaries within the segment). The length of the segment increased as a function of its stream order, ranging from 120 m to up to 882 m for the segments of stream order 2 and 5, respectively. For simplicity, two order-2 streams draining similar catchment areas (2.43 and 2.27 km^2) were averaged to represent a single, mean order-2 stream.

Understanding the contribution of all the processes involved in the observed pCO_2 pattern in a stream network, requires the quantification of each flux independently. The following sections provide a description of the sampling, sample storage and analyses needed to quantify the components involved in the full CO_2 mass-balance: ***a)*** the upstream import of CO_2 (f_R), ***b)*** the external CO_2 soil inputs (f_s), ***c)*** the C emissions (f_e) and ***d)*** the *in situ* net ecosystem metabolism (f_m).

2.3.3. Sampling protocol, frequency and analytical methods

Stream properties were determined directly on site, by measuring the river width, depth and water velocity, the latter using a flow velocimeter (FlowTracker, handheld Acoustic Doppler Velocimeter, ADV, San Diego, USA). River discharge (Q, $m^3\ s^{-1}$) was then calculated using the so-called *mid-section method* (Turnipseed and Sauer, 2010), by assuming a rectangular cross-section shape for these streams. Ambient water parameters, including water temperature (± 0.15 °C), pH (± 0.2), conductivity (± 0.001

mS cm^{-1}), and dissolved oxygen concentration (± 0.2 mg L^{-1}) were measured *in situ* using a multi-parameter probe (600XLV2-M, Yellow Springs Instruments, Yellow Springs, OH) for both stream and soil waters.

The procedure was to sample first down- and then up-stream in each of the segments. Stream water samples were collected in the middle of the channel to obtain a representative sample; soil water samples were obtained from adjacent soils to the channel as described below. The following methods were applied similarly to both stream and soil waters.

Water samples were collected for analyses of dissolved CO_2, dissolved organic carbon (DOC) and dissolved inorganic carbon (DIC) as well as for water isotopes (^2H, ^{18}O). Samples for dissolved gas concentrations were obtained using a headspace equilibration technique (McAullife 1971, Hope et *al.,* 1995, Sobek et *al.,* 2003), performed as follows. Water was collected in 1 L sealed glass bottles, from which 400 mL was pumped out to create a headspace filled with ambient air. The bottles were then shaken for two minutes to allow the equilibration between the water and the headspace. The equilibrated headspace air was then pumped into air-tight aluminum gas bags by re-injecting the water into the bottle. The CO_2 concentration in the headspace air was later measured in the lab using a gas analyzer (UGGA, Los Gatos Research, Inc.; DLT 100, St Clara, USA, precision of 0.1 - 1 % depending on measured concentration). At each site, reference air samples were also analyzed for later concentration calculations. The concentrations of CO_2 within the water phase could then be retrieved by following Henry's law (Weiss, 1974), which mostly depends on both *in situ* and post-shaking temperatures, gas solubility (Butler, 1982) and the headspace-water ratio.

Water samples for DOC and DIC analyses were first filtered (0.45 µm PES cartridge, Sarstedt AG & co, Nümbrecht, Germany) into acid-washed air-tight vials and stored in the dark at -3 °C pending analysis. Once back in Montreal, water samples were analyzed using a Total Organic Carbon analyzer (Aurora 1030, OI Analytical, College Station, TX, precision 0.05 mg L^{-1}), which allowed us to get both DIC (via acidification) and DOC concentrations (through combustion). Water samples for water isotope (^{18}O and ^{2}H) analysis were collected in 30 mL Nalgene bottles, making sure there were no bubbles in the bottle, then left at room temperature until analysis. Isotopic analysis of water was conducted using a laser spectroscopic technique of liquid water (LGR DT-100 Liquid Water Stable Isotope Analyzer, Los Gatos Research Inc., CA, US). The d-excess ratio was derived from these 2 water isotopes as $d - excess = \partial^2 H - \partial^{18} O \times 8$ (see Supplementary Information A.1 for further details). Water was also collected into pre-rinsed 2 L Nalgene sampling bottles, stored into a cooler for total alkalinity measurements that were performed later in the lab. Total alkalinity was measured based on the potentiometric titration method for low alkalinities, using hydrochloric acid (0.1 N HCl) to a fixed end-point pH of 4.5, following the procedure of the American Society for testing and materials (1982).

2.3.3.1. Lateral inputs, *fs*

Lateral inputs designate the flux of external water entering the stream associated to the simultaneous delivery of soil-derived CO_2 and DOC. Lateral inputs were calculated as the product of lateral water discharge and the concentrations of CO_2 and DOC.

La Petite Romaine stream network consists of small to medium-sized streams (order 1 to 5) tightly connected to the surrounding riparian zone, inducing interactions between underground aquifers and surface water. This exchange or flux referred to as "lateral water inputs" to the stream channel addresses both the subsurface (soil water)

and groundwater inputs (vertical inputs). The relatively low slopes and well-drained soils of this watershed provide good conditions for infiltration of precipitation (rainfall and snowmelt) that rapidly penetrate through the soil to reach groundwater, leading to low rates of surface runoff, which we will therefore discard from our water budget. The lateral water discharge to a given segment was inferred from the change in discharge within each segment, assuming that there was neither precipitation nor evaporation occurring at the time of sampling within the segment, such that the difference between the stream water discharge at the end of the segment (Q_O) and at the top (Q_R) was the lateral water discharging to the stream: (Q_{GW}, $m^3\ s^{-1} = Q_O - Q_R$). The challenge with this calculation is to robustly quantify the small changes that occur in discharge within the short segments that we are working with. In order to estimate this parameter, we developed an empirical model that predicts discharge at any given point based on the relationship between our measured discharge and the estimated flow accumulation at each site, an approach previously used by Rasilo et *al.,* in 2017 and Hutchins et *al.,* in 2017. We developed separate models for spring and for summer flow conditions (see Supplementary Information A.3 and Figure A.1 for further information).

To sample the soil waters that make up the lateral water inputs, three to five custom-made PVC piezometers were set at proximity of the streams (50 to 150 cm) whenever logistically feasible. Piezometers were purged twice, and then allowed to fill; a floating Styrofoam ball was added to minimize gas exchange while filling. Sampling was carried out with a peristaltic pump (MasterFlex 7518-12, Cole-Parmer Instrument Company, Vernon Hills, IL). The measurements were taken in a separate graduated cylinder for soil water, when the probe could not be immersed directly in the piezometers. The water samples (minimum 0.75 L of soil water) were stored and then transported in a cooler to the laboratory for further analyses. Similar analyses to stream were made on soil waters.

2.3.3.2. CO_2 emissions (f_e) and gas exchange coefficient (k_{600})

The CO_2 emission flux (f_e) was estimated by solving a CO_2 mass balance for each segment as follows:

$$f_e = f_R + f_s - f_o \pm f_m$$

Where f_o is the downstream export of CO_2, f_R is the upstream import of CO_2, f_s is the external input of CO_2 from soils, and f_m is the *in situ* net ecosystem metabolism.

In addition, we quantified stream CO_2 emissions (f_e) using short-term (5 min) floating chamber measurements in the up and downstream sites of each segment. To represent the morphological and hydraulic heterogeneity of the stream, chamber measurements were done in both low (pools) and high-turbulence areas (riffles) in each site and subsequently averaged. The instantaneous CO_2 accumulation in the chamber headspace over time was measured with an ultraportable greenhouse gas analyzer (Los Gatos Research, Inc.; DLT 100, St Clara, USA) directly connected to the chamber in a closed loop. Flux measurements (f_e, g C m^{-2} d^{-1}) were then derived from the slope of CO_2 increase over time within the chamber headspace (Muller et *al.*, 2015, Supplementary Information A.2, Table B.1).

Both the mass balance and the flux chambers were used to calculate the gas exchange coefficient (k_{CO_2}, m d^{-1}) using Fick's first law of diffusion based on the gradient of CO_2 concentration between the water surface and the atmosphere. Then k_{CO_2} was converted to k_{600} using the Schmidt number with an exponent of 0.5 (Supplementary Information A.2, Table B.2). For comparative purposes, we also used published empirical models to calculate a k_{600} for each segment and season based on stream

geomorphology (Raymond et *al.,* 2012, Natchimuthu et *al.,* 2017, Ulseth et *al.,* 2019) (Supplementary Table B.2).

2.3.3.3. Stream metabolism, f_m

Stream whole-ecosystem metabolism was measured in two different segments (LR2a, LR2b) as Net Ecosystem Production (NEP) based on diel shifts in dissolved oxygen in stream water (Supplementary Table B.1). NEP represents the imbalance between gross primary production (GPP) and ecosystem respiration (ER). Thus, stream metabolism is a net source of CO_2 when ecosystem respiration exceeds gross primary production (*i.e.* NEP < 0). To measure diel dissolved oxygen dynamics, we deployed one miniDOT logging sensor (PME Inc., Vista, California, USA) in each of the two segments, above the stream bed with a rigid rod, such that the logger was able to move freely with the current. The variations of water level, O_2 and temperature were recorded every 10 min, for 1 month (from end of June 2016 to beginning of August 2016). We assumed a 1:1 molar conversion between O_2 and CO_2. We derived NEP value using a maximum likelihood model, returning the best combination of GPP and ER with the least difference between the modeled and the measured sensor O_2 (Hall and Hotchkiss, 2017, see further details on the methodology in Supplementary Information A.4).

2.3.4. Assessing the influence of each process to stream CO_2 (f_R) dynamics along a fluvial network

The overall objective of this study was to assess how the various processes involved in stream CO_2 dynamics combine to determine the declining pattern observed along riverine network. To do so, we first calculated the relative contribution of each process to the change in the riverine CO_2 flux along each segment (*i.e.* the difference between f_O and f_R). We calculated the relative contribution of soil CO_2 inputs, metabolism and emissions to the change in riverine CO_2 flux by dividing each process-derived flux by the sum of all of them. For example, the percent relative contribution of soil CO_2 inputs

was calculated as $\frac{f_s}{f_s+f_m+f_e} \times 100$. To assess whether our CO_2 mass balance yielded reasonable solutions for each segment and season, we compared the gas exchange coefficient (k_{600}) that would satisfy the principle of mass conservation with measured and other modeled k_{600} values. If our mass balance-derived k_{600} values were not comparable to those derived from both chambers and published empirical models, we discarded that particular segment and season from further analyses. A large mismatch between the k_{600} solutions of the mass balance and the observed and modeled k_{600} might indicate unaccounted processes (*e.g.* photodegradation and methane oxidation), or/and that one or several of the fluxes were not accurately estimated.

In addition, we calculated the impact that each process has on the riverine CO_2 flux (f_R = discharge × CO_2 concentration) at any individual point along the La Romaine stream continuum. The contribution of each process depends on its magnitude (*i.e.* the mass of CO_2 per unit time that each process is adding or removing from the stream) but also on the magnitude of the riverine CO_2 flux itself (*i.e.* the mass of CO_2 per unit of time that the stream is already transporting). We define the impact that CO_2 emissions have on riverine CO_2 fluxes ($K_{fCO_{2e}}$, km^{-1}) as:

$$K_{fCO_{2e}} = \frac{f_e}{f_R} \times \frac{1}{x}$$

Where x (km) represents the length of the stream segment that the emission flux (f_e) is referred to. Likewise, the impact that NEP has on the riverine CO_2 flux (K_{NEP}, km^{-1}) is calculated as:

$$K_{NEP} = \frac{f_m}{f_R} \times \frac{1}{x}$$

Finally, the impact that soil-derived CO_2 inputs has on the riverine CO_2 flux ($K_{fCO_{2s}}$; km^{-1}) is calculated as:

$$K_{fCO_{2s}} = \frac{f_s}{f_R} \times \frac{1}{x}$$

These contribution values (K), expressed on a stream length basis, can be interpreted as a potential turnover rate of CO_2 due to each process and allow us to place these processes within a broader CO_2 dynamic at the fluvial network scale. For example, a $K_{fCO_{2s}}$ of 1 km^{-1} would imply that, within that given portion of the network, the soil water inputs alone would increase stream CO_2 concentrations by twofold within a stretch of a kilometre. All statistical analyses were conducted on R 1.0.136 and Jump 13 Pro.

2.4. Results

2.4.1. General stream conditions

We observed seasonal variability between our June and August samplings mostly in discharge (Supplementary Fig. A.1) and temperature (not shown here), but less so for surface water pCO_2 (Fig. 2.2) and DOC (data not shown). Overall, the spatial variability along the fluvial continuum was greater than the variability between years, thus we will focus on the average of both 2015 - 2016 in all our variables. Mean O_2 values varied between 10.19 ± 1.11 to 8.87 ± 1.25 mg L^{-1} in stream water, decreasing from the 1st stream segment to larger streams (Supplementary Table B.3) and was overall higher in spring compared to summer (10.48 and 8.83 mg L^{-1} respectively). Soil waters displayed a significant variability in O_2, with concentrations ranging from 4.31 ± 3.35 to 8.42 ± 3.33 mg L^{-1} (or 40 to 70 % of O_2 saturation), and no significant spatial trend was found. It is important to note that soil waters were mostly oxic, with an average of 6.26 mg L^{-1} (58 % of saturation). DIC concentrations in streams reached 0.92 ± 0.11 mg C L^{-1} in spring and 1.27 ± 0.30 mg C L^{-1} in summer, whereas soil waters had always higher DIC concentrations (on average *c.a.* 5 times). Our sites were characterized by an overall low conductivity, slightly increasing with stream order, from an average 9 µS cm^{-1} in the 1st segment to 11 ± 0.9 µS cm^{-1} downstream, as well as a slightly acidic pH increasing with stream order. In this regard, bicarbonate (HCO_3^-) ions were not considered in our mass balance, since the low average pH suggested that CO_2 was the predominant species (> 50 % of total DIC). However, higher stream water pH in larger streams point to a somewhat larger role of bicarbonate downstream.

All sampled streams in *La Petite Romaine* river network were supersaturated in CO_2, and there was a large degree of spatial variability in CO_2 partial pressure both within and across sites. Overall pCO_2 was declining along the continuum, ranging from 2 398 ± 537 µatm SD in the headwaters (source) to 687 ± 138 µatm SD downstream, with a stronger decrease occurring from orders 1 to 4 (headwaters to seg # 2) (Fig. 2.2, Supplementary Table B.3). Although this spatial pattern was present in both spring and summer, it was more pronounced in summer (average of 1 083 ± 709 µatm) compared to the spring season (average of 855 ± 530 µatm). This declining trend in stream pCO_2, which has already been observed in other stream networks (*e.g.* Deirmendjian and Abril, 2018, Venkiteswaran et *al.*, 2014, Doctor et *al.*, 2007, Wallin et *al.*, 2012), is the pattern we attempted to better characterize and understand in this study.

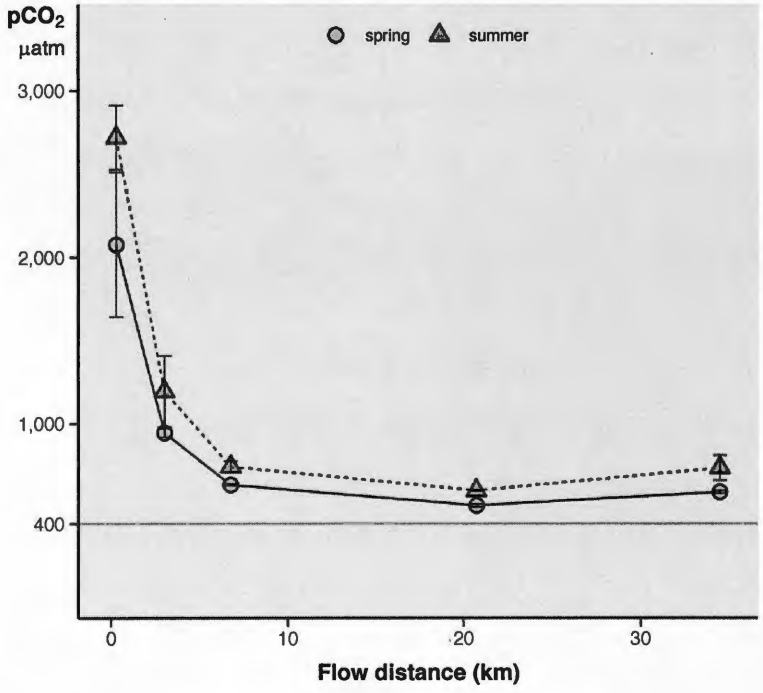

Figure 2.2 Seasonal and spatial stream pCO_2 (µatm) variability across the fluvial network of *La Petite Romaine,* ranging in size from headwaters to stream of strahler order 5 (from left to right). The triangles and circles represent the measured pCO_2 values in Spring and Summer respectively. This is the spatial pattern is the one we aim to better understand.

2.4.2. Network patterns of measured processes and fluxes

2.4.2.1. The network pattern of lateral inputs, f_s

The soil water pCO_2 values (pCO_2 range = 6 659 to 22 550 µatm) were consistently higher and much more variable than those in the adjacent stream waters (pCO_2 range = 539 to 2 398 µatm) (Fig. 2.3). Likewise, DOC concentrations in soils waters were more variable (range = 6.37 to 14.77 mg L^{-1}) compared to stream waters (4.15 to 7.72 mg L^{-1}) (Fig. 2.3). pCO_2 values in stream waters were on average 13 times lower than in the adjacent soil waters (*i.e.* mean pCO_2 = 969 and 12 140 µatm, respectively), whereas the difference between stream and soil water DOC concentrations was much smaller (*c.a.* 4 times on average). This suggests that whereas these C species present in streams likely originate partly from soil waters, they undergo different processing and transformations along the soil-aquatic continuum. Interestingly, contrary to what was observed for stream water, CO_2 concentrations in soil waters tended to increase towards downstream sites (Fig. 2.3). While soil water DOC did not show any clear pattern downstream in spring, a clear declining trend of soil water DOC was observed along the fluvial continuum in summer (Fig. 2.3).

During the early spring season (*i.e.* the period of snowmelt) the stream discharge ranged from 0.24 to 16.87 $m^3\ s^{-1}$, in the first and last segment, respectively. Similarly, stream discharge ranged from 0.16 to 15.56 $m^3\ s^{-1}$ in summer, when the stream is mostly groundwater-fed. The estimated later water input (Q_L) averaged 4.92×10^{-5} $m^3\ m^{-1}\ s^{-1}$ ($\pm$ 2.82×10^{-5} $m^3\ m^{-1}\ s^{-1}$) and tended to decline downstream the network (Supplementary Table B.3). Although the cumulative lateral water inputs along the segments increased downstream as a function of flow distance (Supplementary Fig. A.1), the log-slope of river discharge as a function of flow distance was much higher than that of Q_L (1.8 vs 1.2), resulting in a decline of the lateral water inputs rates (k_L = km^{-1}, the ratio of lateral flow input per meter of river to total river discharge) with

increasing flow distance (Fig. 2.3). This suggests potential offsets between downstream shifts in lateral water inputs, and in the concentrations of CO_2 and DOC associated to these lateral waters, which eventually determine the net result in terms of riverine CO_2 and DOC concentrations.

The patterns observed with soil C inputs along the network can be related to those of water isotopes. Figure 2.3 shows the spatial distribution of stream water deuterium excess (d-excess), which varies with the degree of water evaporation occurring in the stream, therefore providing some indication of the water residence time within a specific system. Deuterium-excess exhibited a declining trend from the headwaters (15.0 ± 0.4 ‰) to larger streams (13.0 ± 0.6 ‰) similarly in spring and summer seasons. Soil waters displayed high values of d-excess, close to those of local precipitation and to headwater streams, highly connected to soil ecosystems and recent precipitation (not displayed here). But as we move downstream, water ages (*i.e.* subjected to more evaporative enrichment) and lateral water sources become increasingly diluted with aged waters flowing from upstream. These shifts in deuterium-excess reflect changes in the relative age and provenance of the water along the *Petite Romaine* network suggesting that our sites fall along a clear hydrologic flow path that varies in the extent of connectivity to groundwater sources.

2.4.2.2. The network pattern in stream metabolism, f_m

The diurnal O_2 approach yielded consistently negative net ecosystem production (NEP) values, suggesting a systematically higher stream ecosystem respiration relative to system gross primary production (GPP) in *La Petite Romaine* stream network (Supplementary Fig. A.2). The large advantage of this integrative method is that it accounts for the primary production and potential CO_2 uptake within these systems. The two sensors that we deployed in the two streams (order 2), displayed similar patterns of O_2 variation throughout the 30 day-sampling period in August

(Supplementary Fig. A.2). A third sensor that was deployed in the stream of Strahler order 5, displayed highly variable patterns of ambient O_2, which could not be effectively modeled, perhaps due to deployment issues, and was therefore excluded from the final analysis. The two remaining sites, however, showed a high degree of coherence in O_2 dynamics suggesting that O_2 variations in these streams responded to watershed scale drivers, which resulted in a declining trend in NEP with time in both sites (mid-June to end of July, Supplementary Fig. A.2) The two streams were consistently net heterotrophic (negative NEP), and thus a net source of CO_2 to the water column. This average estimate of NEP was similar to the median net CO_2 production rates (0.70 ± 7.05 SD g C m^{-2} d^{-1}) obtained through the difference in DOC concentrations between soil and stream waters, a proxy of in-stream organic matter degradation following Rasilo et *al.,* 2017. While the method based on the difference of DOC concentrations covers all sites for the four sampling periods, the agreement between the two nevertheless suggests that the range of rates obtained realistically capture internal stream CO_2 production. We decided to use the median value of NEP based on diurnal patterns in stream O_2 concentrations, as a baseline for in-stream production of CO_2 in the subsequent mass balance calculations (0.81 ± 0.37 SD g C m^{-2} d^{-1}).

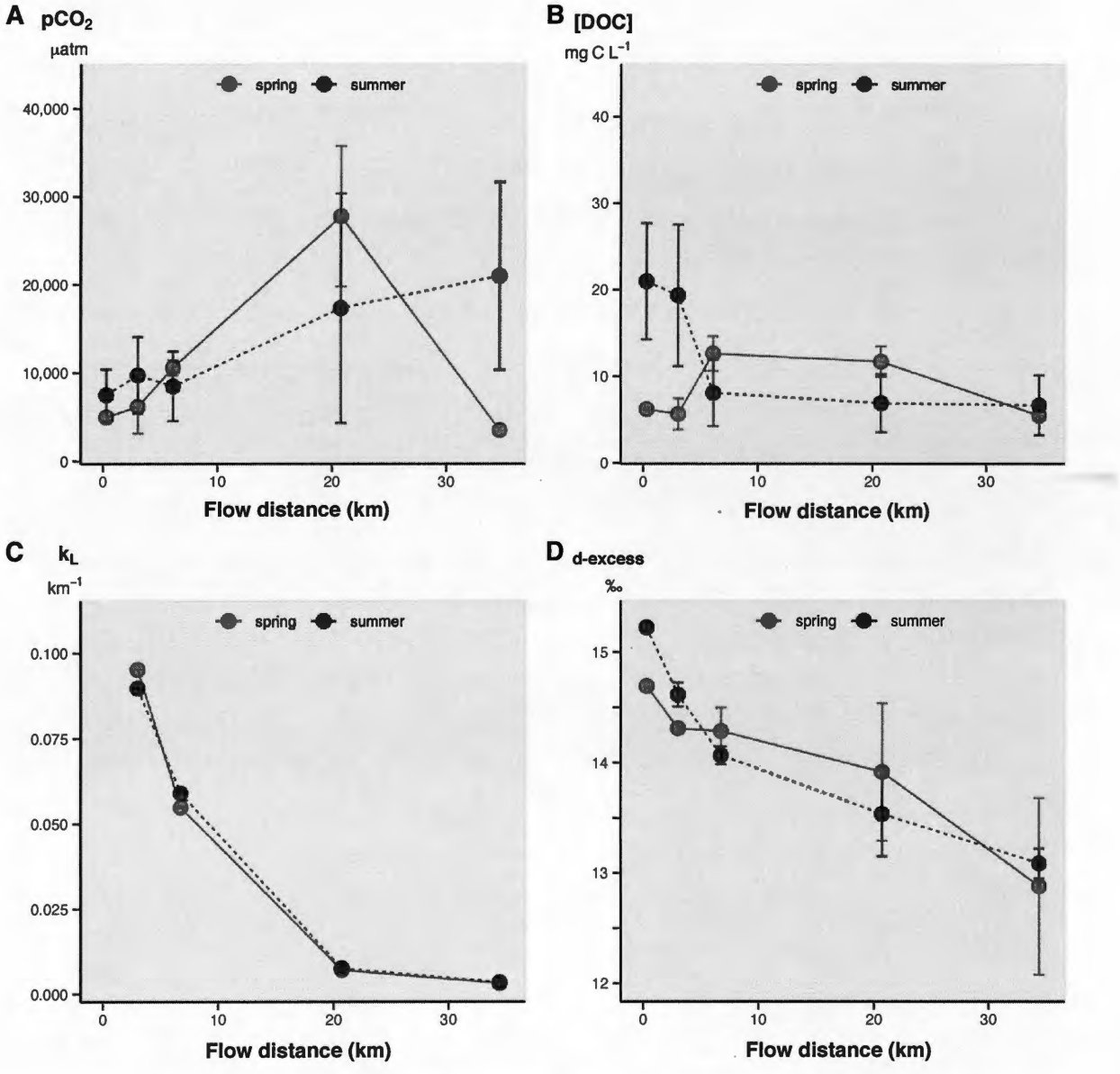

Figure 2.3 Spatial and seasonal soil water contributions to the stream channel of: *a)* soil water pCO_2 (µatm), *b)* soil water DOC concentrations (mg C L^{-1}), *c)* lateral water input per kilometer length of stream (k_L, km^{-1}) and *d)* stream d-excess (‰) as a function of distance from headwaters (= 0 km) to larger streams. *The pale and bright colors indicate samples collected in spring and summer seasons respectively.*

2.4.2.3. The network pattern in gas exchange coefficient, k_{600}

Stream emissions averaged to 1.89 ± 2.67 g C m^{-2} d^{-1} for the entire network, and tended to decline from 4.71 ± 4.77 g C m^{-2} d^{-1} in the 2nd order streams, to 0.79 ± 0.40 g C m^{-2} d^{-1} in our 5th order streams (Supplementary Table B.1). The gas flux at the stream air/water interface is controlled by 2 factors, the first is the CO_2 concentrations gradient between stream water and the atmosphere, and the second, referred to as the gas exchange coefficient (k_{600}), is related to the intensity of gas exchange and driven by physical factors (*e.g.* wind, water turbulence). Although pCO_2 is relatively well constrained in our study sites, the gas exchange coefficient is complex to determine. Our chamber-based k_{600} estimates were similar on average between spring (6.76 ± 1.93 m d^{-1}) and summer (6.84 ± 3.49 m d^{-1}), with an overall network average of 6.80 ± 2.61 m d^{-1} (Fig. 2.4). The standard deviation represented almost 50 % of the actual average value, reflecting a large variability of gas evasion within the network. There was a downstream declining trend in the average gas exchange coefficient along the network, which varied from average values of 9.93 ± 2.35 m d^{-1} SD at the upper stream order to 4.50 ± 0.43 m d^{-1} SD g C m^{-2} d^{-1} at the most downstream segment (Fig. 2.4).

2.4.3. Test of the combination of fluxes to reconstruct the stream k_{600} along the fluvial network of *La Petite Romaine*

In this section, we integrate the processes discussed above within a mass balance context and explore if their combination leads to acceptable gas transfer coefficient solutions. We have carried out an individual mass balance for each of the 4 stream segments along the stream-river continuum, which in the end yield an average predicted k_{600} of 22.82 ± 13.83 m d^{-1}, or 18.45 ± 6.73 m d^{-1} when excluding the outlier in segment 2, in spring (Fig. 2.4, Supplementary Table B.2). In contrast, the k_{600} based on chamber measurement was 6.80 ± 2.61 m d^{-1} on average, which is at least 3 times lower than what our mass balance returns. Yet, using empirical models based on slope

and stream velocity (Raymond et *al.,* 2012, Natchimuthu et *al.,* 2017, Ulseth et *al.,* 2019), the average k_{600} of 9.01 ± 0.99 m d^{-1} lies above our measured k_{600} and below our predicted k_{600} from the mass balance (Fig. 2.4). Despite this difference in magnitude, the 3 methods showed relatively similar declining spatial pattern across the 4 segments, from the headwaters to streams of Strahler order 5. Headwaters showed high mass balance-based-k_{600} (25.61 ± 2.59 m d^{-1}), which tended to decline with flow distance (10.29 ± 1.07 m d^{-1} in segment of order 4). The measured k_{600} decreased smoothly, from 9.93 ± 2.35 to 4.50 ± 0.43 m d^{-1}, whereas the empirical-model-based approach led to a steep spatial decline, similar for all the models, starting from an average of 15.51 ± 2.14 m d^{-1} in the headwaters to 2.88 ± 0.28 m d^{-1} in the largest studied stream, for Natchimuthu et *al.,* 2017, Raymond et *al.,* 2012 and Ulseth et *al.,* 2019.

Overall, the gas transfer coefficient showed higher average values in spring (28.80 ± 17.81 m d^{-1} and 9.75 ± 3.61 m d^{-1}) compared to the summer season (16.84 ± 5.82 m d^{-1} and 8.28 ± 2.47 m d^{-1}) (Fig. 2.4, Supplementary Table B.2) for both the C mass balance and the empirical models, respectively. In contrast, the measured k_{600} showed similar averages in spring (6.76 ± 1.93 m d^{-1}) and summer (6.84 ± 3.49 m d^{-1}). We note the high standard error value of k_{600} in spring calculated via the C mass balance method (± 17.81 m d^{-1}), caused by an extreme spring k_{600} value found in segment 2 (53.39 m d^{-1}). By discarding it, the spring average k_{600} and its uncertainty drop to 20.61 ± 8.53 m d^{-1}.

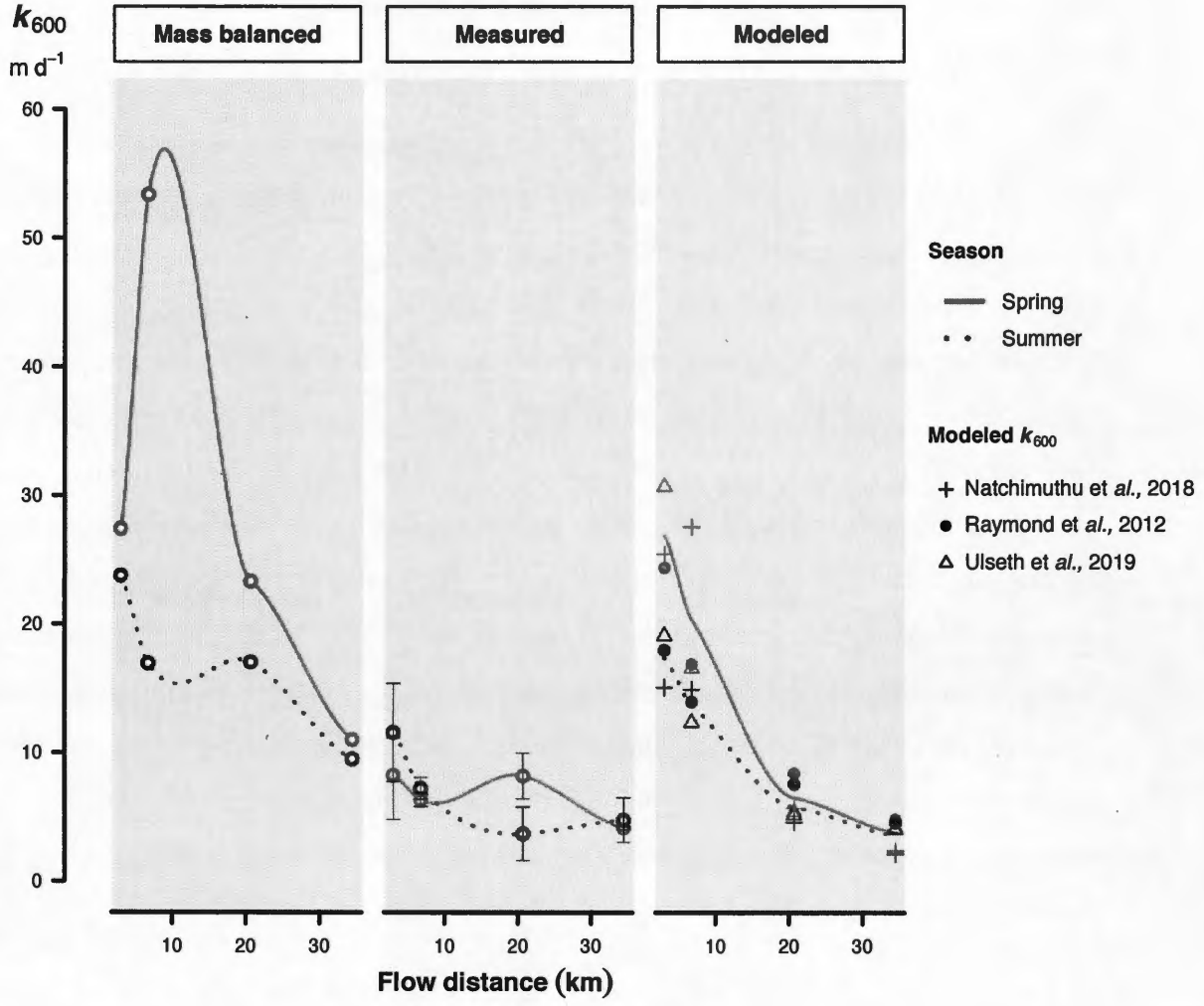

Figure 2.4 Spatial distribution of the gas transfer velocity (k_{600}, m d^{-1}) estimated using 4 different methods, from left to right: *a)* CO_2 mass balance, *b)* floating chambers (average values over 2 years: 2015-2016), *c)* empirical equation of Natchimuthu et *al.*, 2017, empirical equation n°6 Raymond et *al.*, 2012 and Ulseth et *al.*, 2019. *The pale and bright colors indicate samples collected in spring and summer seasons respectively.*

2.4.4. Contribution of different pathways to CO_2 dynamics

2.4.4.1. Contribution of different pathways to CO_2 dynamics at the reach scale

We aimed to evaluate the relative contribution of each process in determining the fluvial CO_2 flux (f_R) within each studied segment along the network, using a general mass balance framework (Fig. 2.5). Note that emissions (f_e) were calculated using the mass balance k_{600} solutions (previously calculated) for each segment. The capacity of each of the processes to affect the ambient stream CO_2 flux (f_R) did not seem to vary across season, with only 1.07 times of difference between spring and summer. Yet, their relative contribution was different across segments (Fig. 2.5). In total, emissions were responsible for 50 % of the change in the stream CO_2 flux (f_R) within segments, before soil water inputs and internal metabolism, each contributing to 38 % and 12 % respectively. The contribution of the processes influencing the change in f_R dynamics within segments showed a high spatial variability: the influence of emissions, first predominant in the headwaters, tended to decrease from the first (60 %) to the most downstream segment (47 %), as well as the influence of soil water inputs that slightly decreased from 36 to 32 %, whereas NEP had an increasing effect from segment 1 to 4 (5 to 21 %).

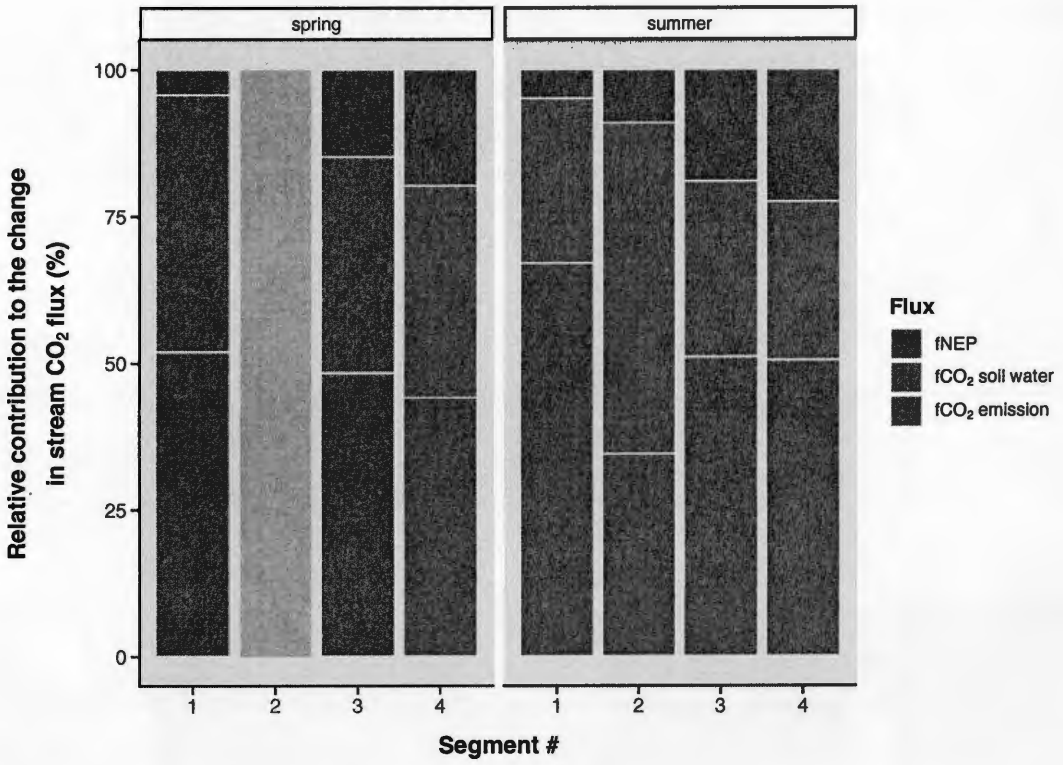

Figure 2.5 Contribution ratio of each flux (NEP, soil water inputs and emissions to the atmosphere) to the change in stream CO_2 flux within each segment, *i.e.* from theoretical upstream to downstream sites (A to B). This is the output plot of the mass balance. Segments # 1 to 4 range from a Strahler order 2 to 4 gradient. The left and right panels represent the Spring and Summer of both 2015-2016. *Spring season data of segment # 2 not displayed here (see explanations in Annex A).*

2.4.4.2. Contribution of different pathways to CO_2 dynamics at the network scale

In the section above, we assessed the CO_2 dynamics at the reach scale. Extrapolating these segments at the network scale (Fig. 2.6) allows to further quantify how the contribution of the main factors influencing riverine CO_2 flux shifts along the riverine network. Figure 2.6 shows the overall average contribution of each process: gas emissions ($K_{f_{CO_{2_e}}}$, using average k_{600} from empirical models for each segment), lateral inputs ($K_{f_{CO_{2_s}}}$) and internal metabolism ($K_{f_{NEP}}$) scaled to the CO_2 mass being transported by the river flow at different points (*i.e.* CO_2 flux, f_R) along the network. In

upstream reaches, soil water inputs and emissions to the atmosphere each represents between 50 to over 60 % of the mass of CO_2 circulating within the river, whereas NEP represents a small contribution (10 %) to the mass of CO_2 transported downstream. Therefore, in these upper reaches, the ambient CO_2 mass undergoes intense turnover within the hypothetical 1-km reach, and appears to be overwhelmingly controlled by external inputs and exchange with the atmosphere. These two processes (emissions and lateral inputs) decline in magnitude downstream relative to the mass of CO_2 that is transported by the river flow, and further converge to the relative contribution of internal production of CO_2, which does not change along the flow path. The 3 pathways stabilize at a value representing roughly 10 % of the CO_2-mass transported downstream by the flow at stream order 5, suggesting that at this point in the network, the external drivers have much less influence on the mass and turnover of the CO_2 transported downriver, and because they tend to cancel each other out, internal processes become the main drivers of ambient pCO_2.

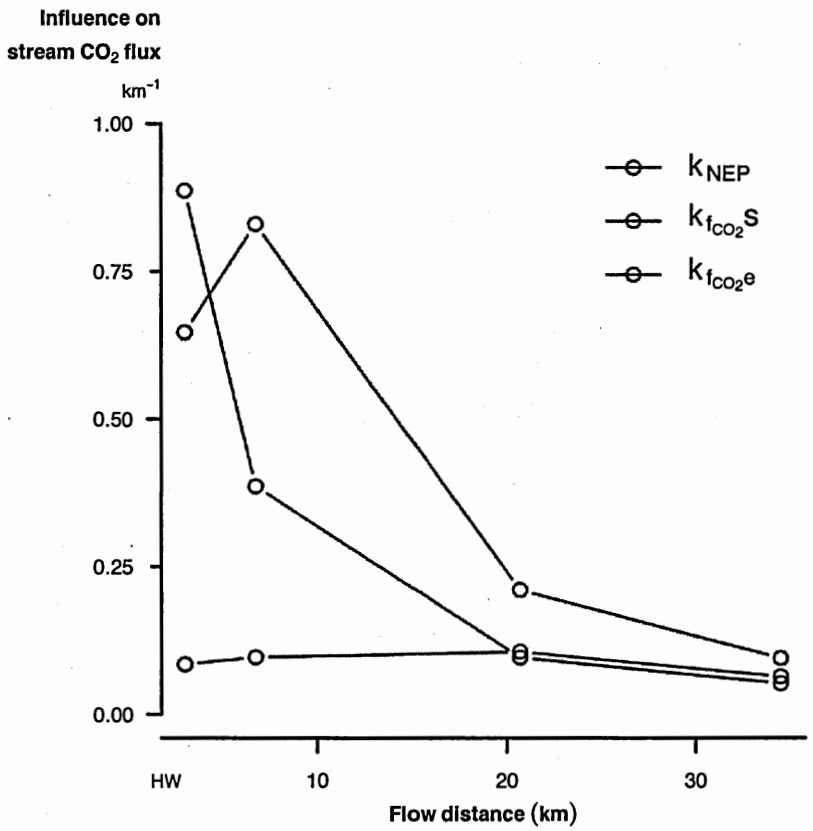

Figure 2.6 Sources and contribution rate per meter length of stream to the stream CO_2 transported downstream declining pattern along a stream-river continuum. The values showed above are averages for spring and summer seasons of both 2015 and 2016. Note that the rate of contribution of CO_2 emissions to the atmosphere (k_{fCO_2e}) was calculated using the gas transfer coefficient (k_{600}, m d^{-1}) based on the average of all the 3 empirical models previously described (Natchimuthu et *al.*, 2017, Raymond et *al.*, 2012, Ulseth et *al.*, 2019).

2.5. Discussion

2.5.1. Network patterns in stream processes

2.5.1.1. General stream features

Although all the studied streams were consistently supersaturated in CO_2 with respect to the atmosphere, they displayed a high degree of spatial and seasonal variability. Ranging from 509 to 2 077 µatm in June (late spring) and from 599 to 2 720 µatm in August, our estimates were lower or in the lower range than those observed in the southern boreal region of Ontario (Canada), which ranged from 1 140 - 3 800 µatm in Spring and 2 280 - 9 500 µatm in Summer (Koprivnjak et *al.,* 2010). Our mean value of 823 µatm is also lower than in other studies of Northern Quebec, which were reported to range from 2 959 µatm from May to October (Campeau et *al.,* 2014), and 1 718 µatm (Rasilo et *al.,* 2017). Yet the range of our pCO_2 values (509 - 2 720 µatm) remained within the broader range of pCO_2 reported in temperate and boreal regions (Wallin et *al.,* 2013) of 360 - 24 000 µatm despite the various seasonal and spatial coverages within the studied dataset. Dissolved organic carbon concentrations in our streams were on average (6.4 ± 1.8 mg C L^{-1}) lower than previously reported in Northern Québec, 9.2 ± 0.7 mg C L^{-1} (Rasilo et *al.,* 2017) and 19.0 mg C L^{-1} (Campeau et *al.,* 2014).

There were no consistent changes in DIC along the flow path, and alkalinity remained relatively low and constant, driven mostly by a rather homogenous regional geology. The decline in pCO_2 observed is not due to a shift in the C equilibrium and pH-driven C speciation, since our own calculations, based on a simple subtraction of the CO_2 from the dissolved inorganic concentration, suggests that only a negligible amount of CO_2 is moved to bicarbonates downstream (not shown here). In these low alkalinity systems where waters tend to be highly supersaturated in CO_2, it is the behaviour of the latter that influences pH, rather than the inverse (Cole and Prairie, 2009).

2.5.1.2. Patterns in stream pCO_2

Although the actual magnitude of pCO_2 varies across networks, the declining pCO_2 pattern with increasing stream order observed in our study is very common, and is not limited to the boreal biome (Teodoru et *al.,* 2009, Finlay 2003, Koprivnjak et *al.,* 2010, Wallin et *al.,* 2011, Campeau et *al.,* 2014, Hotchkiss et *al.,* 2015). Most studies to date have described the pattern and have speculated as to its underlying causes, but few if any has empirically addressed the underlying mechanisms (Lupon et *al.,* 2019, Butman and Raymond, 2011, Hotchkiss et *al.,* 2015). Here, we have identified the main processes responsible for this recurrent spatial pattern in riverine pCO_2 and have further assessed how these processes shift along the network. In order to address both of these questions, we first discuss the individual processes that are involved in this pattern, and then discuss how these various processes combine to yield the observed pattern in stream pCO_2 along the hydrologic continuum.

2.5.1.3. Patterns in lateral inputs

One mechanism that has been extensively reported as the main control over the declining trend in stream pCO_2 is a decrease of soil-derived CO_2 inputs along the network continuum (*e.g.* Marx et *al.,* 2017, Duvert et *al.,* 2018, Hotchkiss et *al.,* 2015, Cole and Caraco, 2001, Polseneare and Abril, 2018, Kokic et a., 2015). A decrease in soil-derived CO_2 inputs might result either from *i)* a decline in the rates of lateral water inputs that carry this soil-derived CO_2, *ii)* a decline in the actual concentrations of CO_2 of these groundwaters that enter the stream, or *iii)* a combination of both. On average, our soil water partial pressure of CO_2 (12 140 ± 10 895 µatm) was in the same range than in another study conducted in a nearby region of Quebec in summer (Rasilo et *al.,* 2017), which reported an average of 10 683 ± 3 221 µatm. Soil water DOC concentrations were lower (11.18 ± 9.22 mg C L^{-1}) than those of that same study (9.7 ± 2.4 mg L^{-1}), as well as in the lower range of DOC values of studies conducted in the

US (Xu et *al.*, 2012, 11 - 35 mg C L^{-1}) and in the Krycklan catchment in Sweden (Kothawala et *al.*, 2015, 20 mg C L^{-1}). The high variability of soil water C concentrations underlies the complexity and the large spatial heterogeneity of the surrounding terrestrial ecosystem along the stream river continuum, further emphasized by a wide range of both pH and conductivity (Supplementary Table B.3). There was, nevertheless, a significant increase in the average concentrations of CO_2 in soil waters moving downstream the network (Fig. 2.3a). This likely reflects a stimulation of biological processes due to an increase in plant cover, soil organic carbon contents and change in landscape features as we move from the barren higher altitude, steep slope regions in the headwaters to the lower altitude, low slope, warmer downstream forested watersheds.

Furthermore, although the absolute amount of lateral discharge to the stream segments increased with increasing stream order, its relative contribution to the total stream flow declined along the flow path (Fig. 2.3c). This is in agreement with the gradual d-excess enrichment observed from small to larger streams, which further indicates: the stronger impact of water evaporation further downstream and the CO_2-rich groundwater inputs increasingly diluted within this large and aged stream water volume (Fig. 2.3d). The modest increase in soil water CO_2 concentrations along the fluvial continuum can therefore not possibly offset the much larger relative decline in lateral water inputs, resulting in an overall net decline in soil-derived CO_2 inputs to the stream, as we have shown in figure 2.6, and which we further discuss below.

2.5.1.4. Patterns in stream metabolism

The net ecosystem production of 0.81 ± 0.37 SD gC m^{-2} d^{-1} for our streams is lower than previously reported in boreal streams (1.12 - 4.66 gC m^{-2} d^{-1}, Lupon et *al.*, 2019, Rocher-Ros et *al.*, 2019). This value, supported by the estimated DOC mineralization (0.70 ± 7.05 g C m^{-2} d^{-1}), suggests that NEP in these streams is supported by the

biological degradation of soil-derived DOC. Several recent studies have used a similar approach based on differences in soil and stream water DOC concentrations (Hutchins et *al.,* 2018, Lupon et *al.,* 2019), and have reported similar ranges in apparent in-stream DOC degradation. The DOC subtraction method yielded highly variable values (coefficient of variation = 1 007 %), which likely reflects the large heterogeneity of the surrounding landcover, the soil organic matter and moisture conditions. Although metabolism cannot possibly explain the spatial decline in ambient pCO_2 by itself, this process may still be responsible for sustaining CO_2 supersaturation in the lower part of the network continuum.

2.5.1.5. Patterns in gas exchange

Although gas concentrations in streams can be relatively well constrained using direct gas measurements in the field, determining the gas exchange coefficient is complex and tedious. Yet deriving robust estimates of gas exchange coefficients is crucial for determining gas emissions and ecosystem metabolism in streams and rivers. We empirically estimated k_{600} using the floating chamber approach and obtained values ranging from 4.60 to 9.80 m d^{-1} across our 4 segments, which is in the lower range of values previously reported in the boreal region of Sweden of 6.50 - 16.10 m d^{-1} (Kokic et *al.,* 2014, Wallin et *al.,* 2018, Natchimuthu et *al.,* 2017), but higher than the average estimate of 3.10 m d^{-1} for boreal stream by Aufdenkampe et *al.* (2011). Although there was no significant relationship between slope (either catchment or stream channel) and k_{600} in our stream network, there was a clear declining trend in gas exchange coefficient along the stream flow path (Fig. 2.4, Supplementary Information A.2), suggesting that small order upstream sites were on average more turbulent than higher order downstream sites, a pattern that has been previously reported (Wallin et *al.,* 2011, 2018, Crawford et *al.,* 2013, Raymond et *al.,* 2013, Butman and Raymond, 2011). The decline in pCO_2 along the fluvial continuum therefore does not seem to result from any

concomitant increase in the intensity of gas exchange, but there is still uncertainty associated to the latter. It is possible that chamber measurements, which can only be carried out in relatively calm reaches, do not reflect the overall gas behavior within the reach, which also includes zones with rapids and more turbulent flow and therefore increased gas exchange coefficient (Attermeyer and Bodmer 2016). Our own comparison (Fig. 2.4) however, suggests overall agreement between chamber-based measurements and modeled gas transfer coefficients, although the former tended to be slightly lower in high slope streams, a pattern that would be expected.

2.5.2. Mass balancing k_{CO_2} along the fluvial continuum

Although the individual behaviour of the various factors within the hydrologic continuum discussed above, provides insight as to their potential role in shaping the observed patterns in ambient stream pCO_2, it is only through integrating their various trends within the context of a complete mass balance that their joint effect can be assessed. The goal was to explicitly determine whether and how the inclusion of various processes improves our ability to close the mass balance and eventually disentangle the observed shift in stream pCO_2 along the network. To do so, we built a mass balance within each of the segments that incorporates all of these measured variables, and which solves for a gas transfer coefficient (k_{600}) that satisfies both observed ambient pCO_2 as well as the measured processes. We took this approach because the stream pCO_2 and other river variables are relatively well constrained, whereas, the gas transfer coefficient is associated to larger uncertainties in terms of its spatial and temporal heterogeneity at the reach or network scale. Acknowledging this, we chose to predict k_{600} from the mass balance instead, and compare the k_{600} solutions to the measured and empirically modeled k_{600} based on stream channel slope and water velocity (Natchimuthu et *al.*, 2017, Raymond et *al.*, 2012, Ulseth et *al.*, 2019), as

alternative approaches to both deriving realistic k values and assessing the robustness of the mass balance solutions.

Although the network patterns in the mass balance k_{600} agreed well with both the measured and the modelled k_{600}, the mass balance k_{600} were on average three-fold higher than the measured k_{600} (Fig. 2.4). The large discrepancy between our chamber measurements, those derived from the C mass balance and published empirical equations based on slope and velocity or from other direct measurements methods, further demonstrates the uncertainty associated with stream gas exchange estimates. All of these approaches may be capturing different facets of gas exchange in these streams, and in addition, each has its own set of uncertainties and limitations. The chamber approach can very accurately quantify k_{600} locally from the changes in ambient pCO_2 within the chamber (lead to good estimates of NEP), but these local values may diverge greatly within the stream (Kokic et *al.,* 2018). In addition, chamber measurements have been criticized for potentially overestimating gas fluxes by causing extra turbulence at the air-water interface (Kremer et *al.,* 2003, Matthews et *al.,* 2003, Lorke et *al.,* 2015), which does not seem the case here since our results were in the lower range of gas exchange values reported (Kokic et *al.,* 2014, Wallin et *al.,* 2018, Natchimuthu et *al.,* 2017). It is more likely that the chamber-based approach underestimates gas exchange velocity for the entire reach.

The mass balance predicted remarkably well the spatial pattern of k_{600} along the stream-river continuum, with good agreement with all the empirical models, displaying a declining pattern towards larger streams (Fig. 2.4). This would therefore suggest that the combination of factors used within our balance captures well the conditions that led to the observed declining pattern in pCO_2 across the fluvial network (Fig. 2.2). This indicates that our mass balance yields reasonable solutions, and that the magnitude and change of the measured variables were well captured.

Note that the seasonal difference observed in the case of the modeled k_{600} (Fig. 2.4) is only caused by an increase in stream velocities (since the only variable used in models is velocity) driven in spring by snowmelt, compared to the baseflow season in summer. In the case of the mass balance, a portion of the seasonal difference in k might be related to the small differences in discharge between the two seasons (Supplementary Fig. A.1), but likely also reflects the compound error associated to the mass balance itself. In spite of this potential error, the mass balance solutions were for the most part very consistent in terms of the magnitude of k_{600} along the network and between seasons. The only major discrepancy that we observed was for the mass balance of segment #2 for spring, which yielded a k_{600} solution that was over two-fold higher than any other k_{600} value in this network, and which was not compatible with the landscape and hydrological features of this stream (*e.g.* low slope, no precipitation within the sampling period). A subsequent sensitivity analysis pointed at an overestimation of soil water inputs within the stream channel as a potential cause for this lack of closure of the mass balance, and the resulting overinflated k_{600}.

The spatiotemporal variability of stable water isotopes (Fig. 2.4d) can be used to allocate water sources of the stream along the network. The shift of the stream water d-excess line at the segment #2 (Fig. 2.3) could indicate a change to more depleted, younger water sources in spring relative to summer. This shift most likely corresponded to the melting of the low elevation snowpack with rising air temperature in spring (Lyon et *al.,* 2018). Our mass balance considers high-CO_2 groundwater as the main lateral source but it would appear that during this period, the main source of lateral water to segment #2 might have been superficial melt water that likely carried lower CO_2 concentration than that we recorded in the groundwater, which explains the lack of closure of the budget for this particular segment in spring, and the subsequent overestimation of k_{600} on the basis of the mass balance. Although our results suggest that a simple mass balance approach that considers lateral groundwater C inputs, stream

NEP and degassing is broadly applicable to reconstruct CO_2 dynamics in this boreal fluvial network, the lack of closure in this segment at this particular time of the year emphasizes the limit of this approach and further highlights the importance of local hydrologic features as well as of seasonal shifts in the pathways of delivery of water and carbon that need to be accounted for.

Previous studies in other boreal regions had reported that the oxidation of soil-derived CH_4 could be a significant pathway fuelling CO_2 supersaturation in small boreal rivers (Rasilo et *al.,* 2017). We did carry out a number of measurements of CH_4 concentration in soil and stream waters, in parallel to those made on CO_2 and DOC, and we found consistently low CH_4 concentrations (data not shown), and importantly, a small difference between soil and stream waters concentrations. We estimate that the oxidation of soil derived CH_4 could not contribute for more than 1% of the observed stream CO_2 fluxes, which is barely discernible from the background noise of variability. For this reason, we decided to exclude CH_4 oxidation as a pathway in order to simplify the mass balance framework.

2.5.3. Influence of the various processes to the fluvial f_{CO_2} dynamics

There has been significant debate within the fluvial research community as to the source of the CO_2 outgassing from the world's rivers (*e.g.* Crawford et *al.,* 2014, Lauerwald et *al.,* 2013, Magin et *al.,* 2017, Venkiteswaran et *al.,* 2014, Leith et *al.,* 2015, Hotchkiss et *al.,* 2015), and recent studies have highlighted the key role that external CO_2 inputs play (*e.g.* Lupon et *al.,* 2019, Marx et *al.,* 2017, Cole and Caraco, 2001, Polseneare and Abril, 2018, Kokic et *al.,* 2015, Duvert et *al.*, 2018). Our results confirm that soil inputs overwhelmingly dominate CO_2 dynamics in small order streams, but further show that their contribution to the ambient CO_2 turnover progressively declines along the flow path (Fig. 2.6), driven by a large decline in the

rates of lateral water inputs (Fig. 2.3). In contrast, the relative contribution of internal metabolism to ambient CO_2 dynamics increased along the continuum (Rocher-Ros et *al.,* 2019). Whereas the contribution of external soil water inputs to CO_2 emissions declined from 89 % to 60 % from stream order 1 to 5, the contribution of internal metabolism increased from 12 % to 40 % along the same flow path. On average, NEP accounted for 24 % of total CO_2 emissions along the entire network up to stream order 5. There are only a handful of studies that can be used for comparative purposes. For example, Hotchkiss et *al.,* (2015) estimated an average contribution of NEP to CO_2 emissions of 28 % across rivers with a much wider range of discharge (0.01 to 100 m^3 s^{-1}). Two other studies (Winterdahl et *al.,* 2016, Rocher Ros et *al.,* 2019) focusing on smaller river have reported a much wider range of contributions of NEP to total riverine CO_2 emissions, from less than 10 % (based on an indirect mass balance approach, Winterdahl et *al.,* 2016) to values ranging between 80 to 182 % (Rocher Ros et *al.,* 2019). Lupon et *al.,* (2019) estimated a contribution of NEP ranging between 11 and 31 % for a small boreal river of order 1 (0.01 m^3 s^{-1}), and this is perhaps the result that is most comparable to ours in terms of being based on a complete mass balance approach. It is clear that the role of NEP varies across networks, and within a given network along the fluvial continuum, but in all cases, it appears to be significant.

Our study was carried out over two distinct hydrologic seasons, *i.e.* during spring snowmelt and summer snow-free season, and although stream CO_2 concentrations were higher in summer, and soil water CO_2, DOC concentrations were lower compared to the spring season, the contribution of the main processes to the network pattern in pCO_2 does not appear to vary significantly from one season to the other (Fig. 2.5).

Overall, our results clearly suggest that whereas soil-derived CO_2 is the dominant factor driving CO_2 dynamics at a reach-scale, it is the combination of external and internal inputs together that explained both CO_2 outgassing and the ambient levels of CO_2 at

the whole network scale. It is also interesting to note that although the rates of internal production of CO_2 were on average much lower than the rates of external loading of soil-derived CO_2, the former become a critical component of the CO_2 balance, determining the position of the plateau of supersaturation that will be attained at the higher stream orders within the network. In the case of *La Petite Romaine* network, this plateau appears to be between 600 and 700 µatm, and subsequent work that our group has carried out in this watershed has confirmed that this plateau is roughly maintained further downstream in order 8 *La Romaine* river (P. del Giorgio personal observation). This value was quite stable within *La Petite Romaine* between the two hydrologic seasons and the two sampling years, suggesting that this steady state balance integrates hydrologic and other watershed features and is therefore characteristic of this fluvial network. Other fluvial networks will likely attain different values of steady state supersaturation in their respective average balances between emission, lateral inputs and internal metabolism. The factors that determine the magnitude of this steady state solution across networks in different landscapes have yet to be explored, and this remains one of the main challenges in our understanding of gas dynamics in fluvial systems. For example, the average pCO_2 in high order rivers (> order 6 strahler) across the boreal biome has been reported to vary between 600 to over 1 000 µatm (Hutchins et *al.,* 2018).

2.6. Acknowledgements

This study was part of the CarBBAS Industrial Research Chair program, co-funded by the National Science and Engineering Research Council of Canada and Hydro Québec. We acknowledge all the members of the CarBBAS group for their help in the field and in the lab, especially Annick St- Pierre, Alice Parkes and Serge Paquet for logistics, and Ryan Hutchins for comments.

APPENDICE A

Supplementary methods

A.1 Water isotopes

Water isotopes are used as a method to infer and further constrain the sources and the processing of water within fluvial ecosystems. The excess of deuterium, or d-excess value reflects the combination of influences from both equilibrium and kinetic effects, generated from water evaporative enrichment and highly depleted soil water inputs respectively. This principle can then be applied to further constrain the spatial variability in the "evaporation to lateral inflow ratio" (= water inputs) within a hydrologic continuum. For example, fast flowing headwater streams that are highly connected to their adjacent soils, tend to have a depleted water isotopic composition similar to the precipitation, whereas as the fluvial network increases in discharge downstream, larger streams are characterized by higher water evaporation, reflected by the progressive buildup of heavy-isotopic ratio in stream water. This divergence of isotopic abundance of a sample from the isotopic abundance of the standard, expressed as the ∂-value, can be quantified by equation (1):

$$\partial^{18}O \text{ or } \partial^{2}H\ (‰) = \left(\frac{R\ sample}{R\ standard} - 1\right) \times 1000 \quad (2)$$

with $R = \frac{heavy\ isotope}{light\ isotope}$

R is the ratio of the heavy to the light isotope of either the sample or the standard signature defined as known composition, such as the water standard SMOW (Standard Mean Ocean Water).

Combining both $\partial^{2}H$ and $\partial^{18}O$ into the deuterium excess (d-excess) parameter (Dansgaard, 1964) as:

$$d - excess\ (‰) = \partial^{2}H - 8 \times \partial^{18}O \quad (3)$$

This d-excess parameter gives indication about water evaporation, such that low d-excess values would reveal a relative isotopic enrichment due to water evaporation.

A.2 Gas emissions, f_e

Diffusive gas emission across the water-air interface ($gC\ m^{-2}\ d^{-1}$) was determined using custom-made foiled floating chamber (ratio area : volume = 172 mm) connected in closed-loop to an infrared gas analyzer (UGGA, Los Gatos Research, Inc.; DLT 100, St Clara, USA), recording continuous (1 sec) pCO_2 in the headspace chamber for 5 min. The initial and final air temperatures in the chamber were also measured, along with the ambient wind speed and wind direction, the atmospheric pressure and water temperature (Kestrel 4500 handheld weather and wind meter, KestrelMeters, Minneapolis, USA). The diffusive CO_2 flux was then calculated according to Fick's law, such that:

$$f_e = \frac{S}{Vm} \times \frac{V}{A} \times \mathrm{T} \times c \quad (4)$$

where f_e is the flux in $\mu mol\ m^{-2}\ d^{-1}$, based on S the rate of the changes in gas over time ($\mu atm\ min^{-1}$), Vm the molar volume ($L\ mol^{-1}$) of a mole of gas used to convert μatm to $\mu mol\ L^{-1}$, $\frac{V}{A}$ the ratio between the volume (V, m^3) and the area (A, m^2) of the floating chamber and T is a conversion factor from min to day (1 d = 1 440 min) and c used for the conversion from $\mu mol\ m^{-2}\ d^{-1}$ to g C m^{-2} d^{-1}.

This constant $c = \frac{Atm\ pressure}{headspace\ temp \times 8.31}$ is function of the atmospheric pressure (kPa), the temperature in the chamber (K) and the universal gas constant (8.31 L atm mol^{-1} K^{-1}).

We used the flux estimate derived from equation (3) (f_e, g C m^{-2} d^{-1}) to derive gas exchange coefficient (k_{CO_2}, m d^{-1}) and the gradient of concentrations between the water surface (CO_2, g C m^{-3}) and the atmosphere (CO_{2a}, g C m^{-3}) both measured, such that:

$$k_{CO_2} = \frac{f_e}{(CO_2 - CO_{2a})} \quad (5)$$

We standardized the gas exchange velocity k_{CO_2} as k_{600}, using the Schmidt number associated with CO_2 gas ($ScCO_2$, Wanninkhof, 1992), with k_{600} at 20 °C (600) and a coefficient of $-1/2$ associated with turbulent waters following the equation developed by Jähne et *al.*, in 1987:

(6) $$k_{600} = k_{CO_2} \times \left(\frac{600}{ScCO_2}\right)^{-1/2}$$

The k_{600} coefficient is also a key variable when estimating metabolism based on an open channel method derived from O_2 dynamics (A.4). Using a Schmidt number associated with O_2 gas (ScO_2, Wanninkhof, 1992), we will determine a gas exchange coefficient specific to O_2.

A.3 Lateral water inputs, Q_L

Lateral groundwater inputs (Q_L) were inferred from the change in discharge within each segment, assuming that within the segment there was neither precipitation nor evaporation occurring at the time of sampling, not additional lateral water inputs from inflowing streams, such that:

(7) $$Q_o = Q_{GW} + Q_R$$

where Q_o = discharge at the end of the segment, in $m^3\ d^{-1}$

Q_R = discharge at the top of the segment, in $m^3\ d^{-1}$

Q_{GW} = groundwater discharge, in $m^3\ d^{-1}$

From this, we derive the lateral water inputs per metre downstream, Q_L ($m^3\ m^{-1}\ d^{-1}$) as:

$Q_L = \frac{Q_{GW}}{x}$.

where x is the length of the segment, in m

The challenge with this calculation is to robustly quantify the small changes that occur in discharge within the short segments that we are working with. In order to estimate

this parameter, we combined actual measurements of stream discharge and theoretical water inputs based on the estimated flow accumulation, an approach previously used in the literature (Rasilo et *al.,* 2017, Hutchins et *al.,* 2007). We determined the flow accumulation for any given point in a stream, which integrates all the area draining that particular point, using the hydrology toolset, ArcGIS). Using a digital elevation model (23 m x 23 m) obtained via GeoBase resources, flow accumulation values were then calculated for each of our sites, by summing all the cells flowing into that particular cell. We then generated a linear regional model of measured discharge at that site versus the estimated flow accumulation, and we did this per sampling campaign. The resulting linear regression models were then used to estimate the relative increase in discharge between the upstream and downstream points predicted on the basis of the increase in flow accumulation between the two sites in each of our segments, and this in turn was used to derive the total groundwater inputs (Q_{gw}, $m^3\ d^{-1}$) and Q_L ($m^3\ m^{-1}\ d^{-1}$), the flow rate per unit of stream length (x). We derived a parameter indicating the relative contribution of these lateral inputs to total discharge, k_L (m^{-1}), calculated as Q_L / Q_o, and we used it to assess whether this relative contribution of lateral water inputs shifted along the hydrologic continuum.

A.4 Stream metabolism and internal production of CO_2, f_m

Stream metabolism focuses on net ecosystem production (NEP), an estimate of the potential *in situ* net CO_2 production or uptake, or the balance between respiration (ER) and photosynthesis (GPP) processes. We assessed the in-stream ecosystem metabolic rate in 3 selected sites based on whole-stream diurnal dissolved oxygen shifts (Hoellein et *al.,* 2013). To do so, we installed three miniO_2 data loggers (PME Inc., Vista, California, USA) at 3 different sites (seg # 2a, 2b, 3), chosen for their relatively easy access, and uniform current pattern. We attached the logger to a rigid metal rod implanted in the stream bed at approximately 30 cm from the bottom, such that the

logger was able to move freely with the direction of the current and also in relation to the water level. We recorded O_2 and temperature data at 10 min intervals, for 1 month (end of June 2016 - beginning of August 2016).

We used the inverse modeling approach proposed by Holtgrieve et *al.*, 2010 to estimate the daily rate of NEP (g O_2 m^{-2} d^{-1}) at each station (Demars et *al.*, 2015), which is summarized in the following equation:

$$(8) \qquad mO_i = mO_{i-1} + \left(\frac{GPP \times PAR_t}{z \times \Sigma PAR} + \frac{ER}{z} + k_{0_2}\,(O_{sat(i-1)} - mO_{i-1})\right)\Delta t$$

where mO_i is the modeled O_2, $\frac{PAR_t}{\Sigma PAR}$ is the relative amount of light (PAR = Photosynthetically Active Radiation, in µmol photons m^{-2} d^{-1}), estimated using geographic coordinates and time (Hall and Hotchkiss 2017), z is average measured stream depth (m), Δt is measurement interval (day).

NEP represents a net consumption or production of O_2 over time (g O_2 m^{-2} d^{-1}). Also, to compare this flux of in g O_2 m^{-2} d^{-1} with our other fluxes in g C m^{-2} d^{-1}, we converted grams of O_2 into grams of C assuming a 1 : 1 molar conversion between O_2 and CO_2.

The approach represented in equation (7) consists in modeling diel changes in dissolved O_2 using the most likely values of GPP and ER in order to best fit the observed O_2 concentration patterns (*i.e.* returning the least difference between modeled and measured dissolved O_2 concentrations). This method is also a way to further assess the quality of our measured estimates (k_{600}, z, O_2, GW inputs) to enable the model to return realistic NEP estimates. The air-water gas exchange coefficient (k_{600}) is particularly important to the final GPP and ER estimates. We therefore included our own measured k_{600} in the model, which allowed us to compare with the ones generated by the model fit in order to assess coherence between the two. We note that the temporal variability of the gas exchange (k_{600}) was low for the measured and modeled values in

our sites, which tends to narrow down some of the uncertainty of estimates of metabolism at these 3 sites.

Deviations from the initial assumptions of the model can also lead to a source of unrealistic estimates of metabolism and increased uncertainty (Demars et *al.*, 2015), in particular: *1)* that no photosynthesis occurs during the night, such that only respiration and gas exchange are responsible for the changes in O_2, and that the resulting night time respiration rates are the same during daytime, and *2)* groundwater inputs are not considered in this model, either as a potential source of O_2 or a potential dilution effect (depleted O_2 water) on stream water.

To avoid adding further uncertainties to the final estimates of NEP, each model output underwent a quality check control on the basis of the following criteria, whereby one step must be validated before moving on to the next: *1)* good visual fit between modeled and measured O_2 distributions (subjective appreciation); *2)* the lowest "negative log likelihood" (nLL) value as possible (-200 was our threshold beyond which we reputed the model), this parameter allows to derive an actual value over the distribution fit; *3)* assessment of plausible ranges of GPP, ER values. We discarded models with positive ER and negative GPP.

In addition, we discarded the first 2 days of probe deployment to allow for the system to settle after the site manipulation, and the final day of the time course, to avoid accounting for the disturbances caused by our presence on site. In one of our sites (seg #3), the iterative model fitting returned consistently poor model fits with unrealistic GPP and ER values, both in magnitude and sign, and extremely large variations of NEP over time, which led us to discard this site. In contrast, the other two sites (segment #2a and 2b) showed very good model fits and returned very plausible ranges of metabolism (*i.e.* median ± range: 1.04 ± 2.08, 0.58 ± 1.31 g C m^{-2} d^{-1} for segment #2a and #2b

respectively), using measured k_{600}, and other geomorphological parameters (stream width, depth). Since PR2a and PR2b were part of a same segment of the same stream order 2, we averaged both to derive a median NEP estimate for La Petite Romaine (0.81 ± 0.37 g C m^{-2} d^{-1}), which we compare with the DOC-based estimate that we describe below.

An alternative approach to quantifying internal stream CO_2 production is to follow the movement of soil-derived DOC into the fluvial network, and to quantify the difference between DOC concentrations in soil water and stream water, following the approach developed by Rasilo et *al.,* 2017 (Fig. A.3). This technique is an alternative perspective of stream metabolism estimation with the one based on diel O_2 changes. Although the approach based on differences between soil water and stream water DOC concentrations yielded a wide range in apparent rates of stream CO_2 production, the average 0.70 ± 7.05 g C m^{-2} d^{-1} matches remarkably well with those estimated based on diurnal patterns of O_2 change.

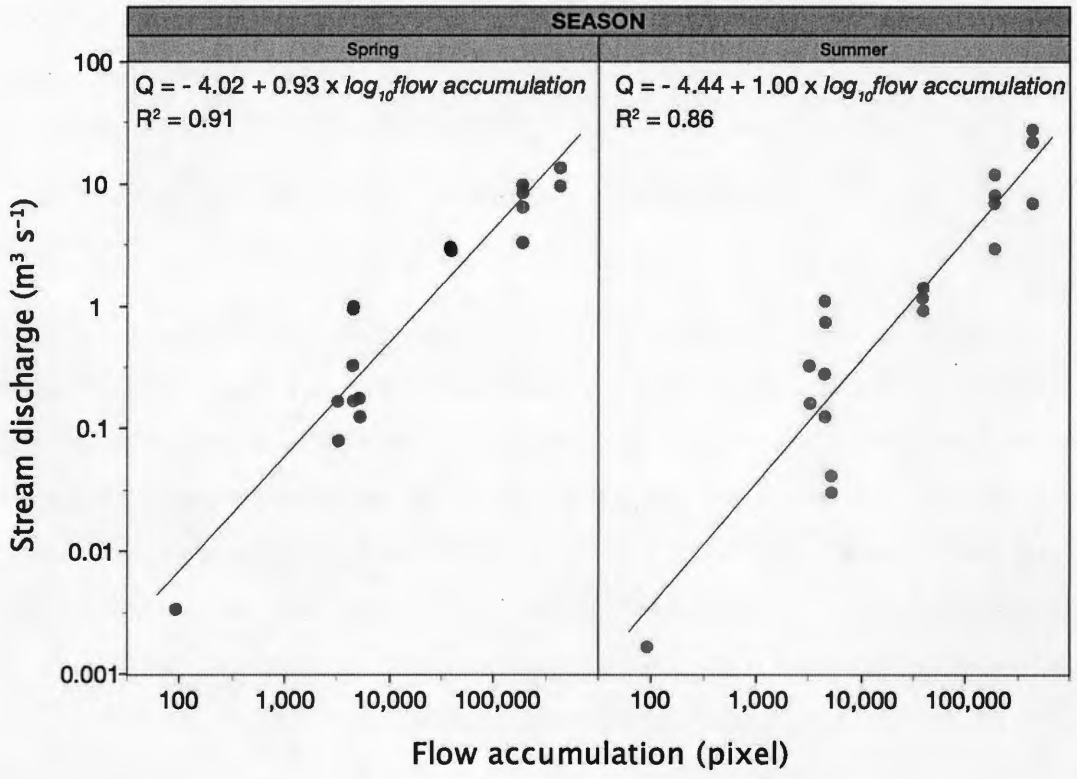

Figure A.1 Log linear regression models based on measured stream water discharge (m^3 s^{-1}) and flow accumulation (pixel, using ArcGIS tool), for both spring and summer hydrological seasons, averaged for 2015 and 2016. The separation over time returned better fits and accounted for the seasonal variations, as June corresponded to high-flows from snowmelt events and August to the base-flow period. The discharge values used and displayed in this study result from the application of these linear regression models on measured data.

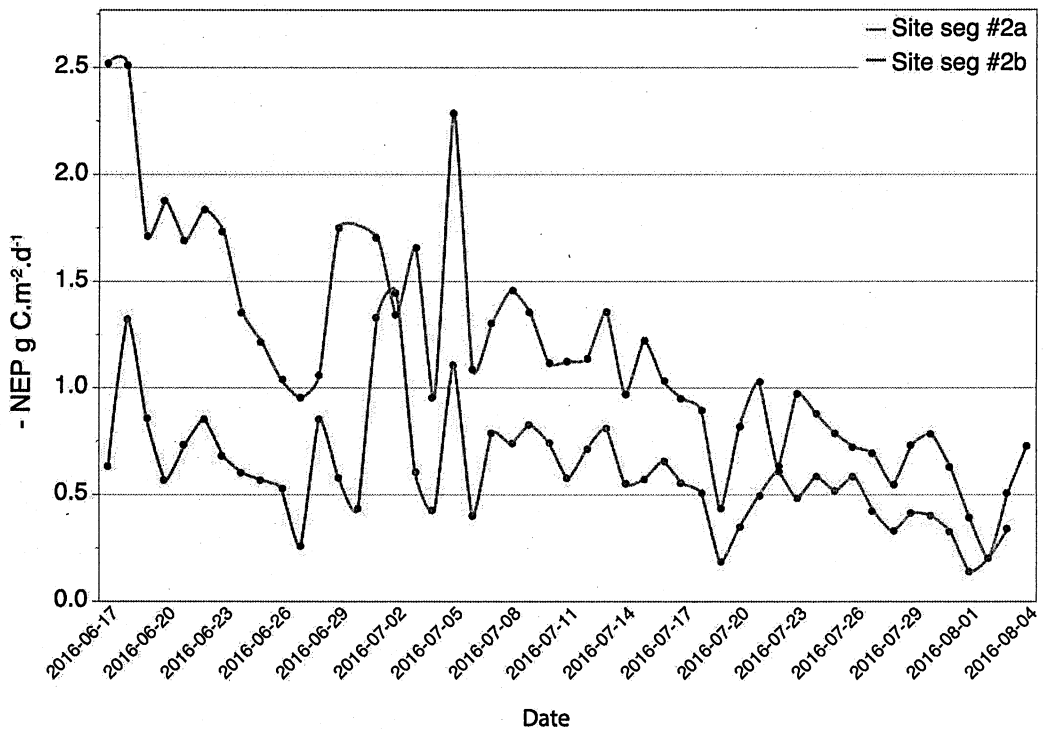

Figure A.2 Time series of the stream net ecosystem production (NEP, g C m^{-2} d^{-1}) in sites 2a and 2b, represented here as -NEP. All the values are positive therefore indicating a net overall system heterotrophy. The higher the values of NEP are, the more the system is balanced towards heterotrophy, seg2b > seg2a.

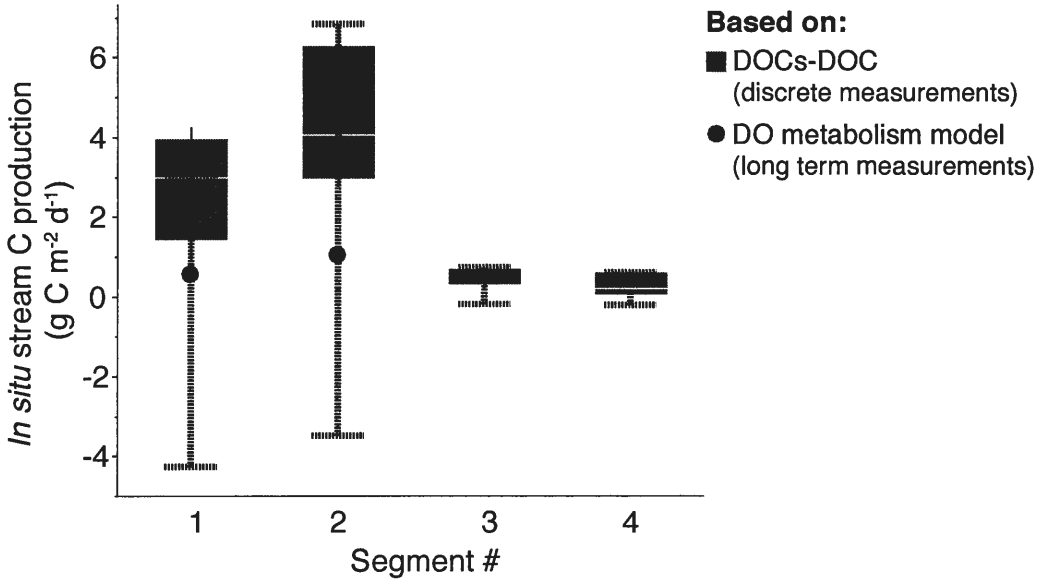

Figure A.3 Internal metabolism estimates for each segment, based on 2 methods: *1)* diurnal O_2 shifts (red dots in the 1st and 2nd segments) and *2)* DOC subtraction between soil and stream systems following Rasilo et al., 2017 (box plots).

APPENDICE B

General framework

The basic mass balance framework considers that CO_2 fluxes for a given segment must be balanced by the combination of upstream inputs, and downstream exports, and in-stream and lateral inputs of CO_2, such that the upstream CO_2 input (f_R), *i.e.* internal processes (f_m) and lateral CO_2 inputs (f_s) must be balanced by the output fluxes, *i.e.* CO_2 emissions (f_e) and downstream CO_2 output (f_o). Then:

(1) $$f_o - f_R = f_e + f_s \pm f_m$$

Note that the appellation f defines a flux, which is the product of a concentration (g C m^{-3}) and a discharge (m^3 d^{-1}) or a rate of gas exchange (m d^{-1}) per stream area (m^2). The CO_2 emissions term (f_e) is the product of the gas exchange coefficient of CO_2 in m d^{-1}, the stream area in m^2 (width, w in m and x the segment length in m) and the gradient of concentrations between atmospheric and stream water CO_2 ($CO_{2_{atm}}$- CO_2, in g C m^{-3}). This term is then written as $k_{CO_2}(CO_{2_{atm}} - CO_2)\,wx$. Note that gas evasion is negative in the equation since our systems are all above saturation. The lateral input flux (f_s) is function of the concentration of C in the soil water entering the streams, as well as the water discharge entering the stream (Q_{GW}). The *in situ* metabolism (f_m) includes the degradation of soil-derived DOM to generate stream CO_2 (+ f_m), and the potential CO_2 uptake via photosynthesis (- f_m). We explored two different cases, the first was to estimate the potential *in situ* production of CO_2 through the degradation of soil-derived DOM, the second was more integrative because it accounted not just for the potential *in situ* respiration but also for in-stream primary production and the balance between the two, referred to as the Net Ecosystem Production (NEP). We used a fixed value because our measurements suggested that there was no discernible pattern with flow distance (see metabolism section above).

We can express the flux of CO_2 downstream (f_o) as the net result of the upstream CO_2 flux (f_R), the lateral CO_2 inputs (f_s) and the CO_2 gas evasion (f_e), such that:

(5) $$CO_{2O}\, Q_O - CO_{2R}\, Q_R = CO_{2_s}\, Q_{GW} + k_{CO_2}\,(CO_{2_{atm}} - CO_2)\, wx + wx\, NEP$$

where Q_{GW} is the lateral water inflow, in $m^3\ d^{-1}$.

We can then use the mass balance to solve for our unknown parameter here, *i.e.* the gas transfer coefficient, k_{CO_2}.

(5) $$k_{CO_2} = \frac{CO_{2O}\, Q_O - CO_{2R}\, Q_R - CO_{2_s}\, Q_{GW} - wx\, NEP}{(CO_{2_{atm}} - CO_2)\, wx}$$

When using the difference between soil and stream water DOC concentration to approximate *in situ* CO_2 production, the following term was tested as an alternative to the NEP term:

$$\alpha = (DOC_s - DOC)\, k_L$$

If photosynthetic uptake were minor in these streams, or if it were roughly balanced by respiration of this autochthonous organic matter, then the two approaches, NEP vs $DOC_s - DOC$ should yield roughly similar rates of *in situ* CO_2 production, and our comparison of both approaches at two sites suggests that this is indeed the case. For simplicity, the final model outputs that we present in the paper contain only the average NEP data (Fig. A.3).

Table B.1 Synthesis table of calculated fluxes based on empirical measurements (segments 1 to 4, from Strahler order 2 to 5). For each one of the 4 segments, values represent averages over 2 years, *i.e.* 2015-2016 and across the 2 sites together delimiting a segment (± standard error). For the variables with seasonal data, spring values are displayed on the left column and summer values are shown on the right column.

		Segment #							
Variables	**Unit**	**1**		**2**		**3**		**4**	
River distance from source	m	3 026		6 772		20 723		34 469	
Segment length	m	120		353		535		882	
Lateral water discharge	$m^3\ m^{-1}\ s^{-1}$	$2.24E^{-05} \pm 6.09E^{-07}$	$1.41E^{-05} \pm 1.62E^{-06}$	$9.75E^{-05} \pm 4.09E^{-06}$	$8.17E^{-05} \pm 3.43E^{-06}$	$5.48E^{-05} \pm$ NA	$5.13E^{-05} \pm 3.83E^{-08}$	$5.32E^{-05} \pm$ NA	$5.35E^{-05} \pm 9.52E^{-07}$
CO_2 evasion flux	$g\ C\ m^{-2}\ d^{-1}$	2.81 ± 2.39	6.13 ± 5.95	1.19 ± 0.16	1.43 ± 0.16	0.91 ± 0.34	0.88 ± 0.3	0.70 ± 0.06	0.84 ± 0.51
CO_2 soil water inputs	$g\ C\ m^{-1}\ d^{-1}$	10.8 ± 7.97	9.95 ± 8.51	67.95 ± 4.53	51.5 ± 21.51	113.49 ± NA	41.64 ± 36.10	13.64 ± NA	74.42 ± 37.97
Net Ecosystem Production	$g\ C\ m^{-2}\ d^{-1}$	0.81 ± 0.37	0.81 ± 0.37	0.81 ± 0.37	0.81 ± 0.37	0.81 ± 0.37	0.81 ± 0.37	0.81 ± 0.37	0.81 ± 0.37

Table B.2 Comparison between gas transfer velocities (k_{600}, in m d^{-1}) obtained through a mass balance approach and the gas transfer velocities derived from empirical measurements (floating chambers), and empirical models found in the literature. The k_{600} calculated from equations in Ulseth et *al.*, 2019 and Natchimuthu et *al.*, 2017 represent both similar streams conditions to our, *i.e.* in small boreal streams. While the third empirical model is a global model applied on headwater streams (equation 6, Raymond et *al.*, 2012). Spring values are displayed on the left column and summer values are shown on the right column.

		Segment #							
Variables	**Unit**	**1**		**2**		**3**		**4**	
River distance from source	m	3 026		6 772		20 723		34 469	
Segment length	m	120		353		535		882	
Mass balanced k_{600}	m d^{-1}	27.44	23.78	53.39	16.97	23.35	17.06	11.04	9.53
Measured k_{600}	m d^{-1}	8.00 ± 6.36	11.59 ± 7.66	6.33 ± 0.99	7.23 ± 1.70	8.23 ± 3.55	3.73 ± 4.16	4.19 ± 0.20	4.80 ± 3.45
Modeled k_{600} (Ulseth et *al.*, 2019)	m d^{-1}	30.70	19.13	16.62	12.38	5.44	5.18	4.19	4.07
Modeled k_{600} (Natchimuthu et *al.*, 2017)	m d^{-1}	25.49	15.10	27.59	14.95	5.72	4.63	2.41	2.18
Modeled k_{600} (Raymond et *al.*, 2012)	m d^{-1}	24.43	18.01	16.92	13.99	8.43	7.58	4.86	4.57

Table B.3 Table summarizing the main variables collected in *La Petite Romaine* stream (above) and soil water (below). Each column represents a different segment number in a growing stream order sequence, from left to right: Seg# 1 < 2 < 3 < 4. Note that the first column is an endmember at the headwaters of La Petite Romaine watershed (not part of the mass balance calculation), and segment # 2 represents the average of 2 segments of same strahler order. Each value represents the average (± standard error) of each of the measured parameters over 2 years, *i.e.* 2015, 2016. Note that for the variables with seasonal data, spring values are displayed in the left column and summer values in the right column.

Stream section features		Segment #										
		/		1		2		3		4		ALL
Strahler order	#	1		2		4		5		5		*mean*
River distance (HW = 0)	m	303		3 026		6 772		20 723		34 469		13 300
Segment length	m	NA		120		353		535		882		428 ± 258
Elevation	m	837		560		588		500		498		574 ± 104
Slope	m m^{-1}	NA		0.024		0.008		0.005		0.003		0.022 ± 0.033
Width	m	0.80		1.28		7.15		27.63		46.40		16.77 ± 17.31
Depth	m	0.23		0.56		0.44		0.84		1.39		0.70 ± 0.37
Stream water discharge	m^3 s^{-1}	6.0E^{-03} ± NA	3.0E^{-03} ± NA	2.4E^{-01} ± 0.03	1.6E^{-01} ± 0.02	1.8 ± 0.02	1.4 ± 0.02	7.8 ± 0.02	6.7 ± 0.02	16.9 ± 0.03	15.6 ± 0.03	5.0 ± 5.90
Lateral water discharge	m^3 m^{-1} s^{-1}	2.1E^{-05} ± NA	1.1E^{-05} ± NA	2.2E^{-05} ± 6.1E^{-07}	1.4E^{-05} ± 1.6E^{-06}	9.8E^{-05} ± 4.1E^{-06}	8.2E^{-05} ± 3.4E^{-06}	5.5E^{-05} ± NA	5.1E^{-05} ± 3.8E^{-08}	5.3E^{-05} ± NA	5.4E^{-05} ± 9.5E^{-07}	4.92E^{-05} ± 2.82E^{-05}
Measured k_{600}	m d^{-1}	1.73 ± 1.99	1.18 ± 1.13	8.00 ± 6.36	11.59 ± 7.66	6.33 ± 0.99	7.23 ± 1.70	8.23 ± 3.55	3.73 ± 4.16	4.19 ± 0.20	4.80 ± 3.45	6.29 ± 4.67

Stream water		Segment #										
		/		1		2		3		4		ALL
Strahler order	#	1		2		4		5		5		*mean*
pH	/	5.28 ± 0.03	5.04 ± 0.02	5.81 ± 0.31	5.95 ± 0.33	6.33 ± 0.31	6.41 ± 0.12	6.38 ± 0.19	6.48 ± 0.26	6.34 ± 1.51	6.35 ± 0.51	**6.11 ± 0.56**
Conductivity	µS cm^{-1}	6.0 ± NA	7.3 ± 0.4	8.0 ± 0.4	10.1 ± 0.1	7.5 ± 0.6	10.3 ± 1.1	8.5 ± 0.6	10.0 ± 1.2	11.0 ± 2.8	11.2 ± 0.4	**9.1 ± 1.7**
O_2	mg L^{-1}	9.04 ± 1.31	8 ± 0.47	10.73 ± 1.01	9.64 ± 1.01	10.99 ± 2.02	8.89 ± 0.44	11.24 ± 0.60	8.5 ± 0.49	9.68 ± 0.97	8.46 ± 1.28	**9.63 ± 1.46**
O_2 saturation	%	94 ± 6	91 ± 6	90 ± 9	92 ± 10	95 ± 15	91 ± 4	102 ± 1	88 ± 4	84 ± 19	88 ± 14	**92 ± 10**
pCO_2	µatm	2 077 ± 614	2 720 ± 272	945 ± 50	1 195 ± 429	633 ± 10	743 ± 66	509 ± 20	599 ± 5	591 ± 12	736 ± 150	**969 ± 626**
CO_2	mg C L^{-1}	1.23 ± 0.36	1.41 ± 0.14	0.72 ± 0.04	0.76 ± 0.27	0.46 ± 0.01	0.43 ± 0.04	0.34 ± 0.01	0.33 ± 0.00	0.43 ± 0.01	0.40 ± 0.08	**0.60 ± 0.34**
DIC	mg C L^{-1}	1.66 ± 0.74	1.27 ± 0.30	1.45 ± 0.49	1.40 ± 0.62	0.92 ± 0.11	1.03 ± 0.28	1.24 ± 0.69	1.12 ± 0.73	1.03 ± 0.03	0.84 ± 0.19	**1.17 ± 0.49**
DOC	mg C L^{-1}	4.21 ± 0.19	5.79 ± 1.45	7.6 ± 0.46	7.19 ± 2.14	5.17 ± 0.59	4.15 ± 0.82	7.71 ± 1.86	6.71 ± 1.73	6.00 ± 0.49	7.48 ± 1.56	**6.36 ± 1.77**
NEP	g C m^{-2} d^{-1}	0.81 ± 0.37	0.81 ± 0.37	0.81 ± 0.37	0.81 ± 0.37	0.81 ± 0.37	0.81 ± 0.37	0.81 ± 0.37	0.81 ± 0.37	0.81 ± 0.37	0.81 ± 0.37	**0.81 ± 0.37**
d-excess	‰	14.69 ± 0.51	15.22 ± 0.11	14.31 ± 1.16	14.62 ± 0.41	14.29 ± 0.54	14.07 ± 0.64	13.92 ± 1.03	13.54 ± 0.86	12.88 ± 1.13	13.09 ± 0.46	**14.03 ± 0.91**

Soil water		Segment #										
		/		1		2		3		4		ALL
Strahler order	#	1		2		4		5		5		*mean*
pH	/	5.23 ± NA	5.09 ± 0.41	5.67 ± 0.41	6.01 ± 0.60	6.11 ± 0.29	5.66 ± 0.24	5.88 ± 0.19	5.66 ± 0.39	5.27 ± NA	5.31 ± 0.09	**5.67 ± 0.45**
Conductivity	µS cm^{-1}	8.0 ± NA	17.5 ± 6.4	44.0 ± 26.0	31.6 ± 21.4	33.5 ± 31.8	18.3 ± 2.5	28.5 ± 17.7	24.5 ± 5.0	13 ± NA	41.3 ± 24.6	**29.0 ± 18.9**
O_2	mg L^{-1}	7.84 ± NA	4.91 ± 2.53	9.41 ± 1.33	7.43 ± 5.32	7.49 ± 1.81	4.38 ± 3.94	6.45 ± 6.3	2.16 ± 0.39	9.00 ± NA	4.23 ± 0.60	**6.26 ± 3.51**
O_2 saturation	%	91 ± NA	55 ± 30	81 ± 12	74 ± 56	66 ± 18	44 ± 41	57 ± 55	23 ± 5	41 ± NA	43 ± 5	**58 ± 33**
pCO_2	µatm	4 991 ± NA	7 493 ± 4 118	6 172 ± 5 247	9 739 ± 8 645	10 577 ± 1 518	8 483 ± 6 828	27 756 ± 13 826	17 345 ± 18 408	3 502 ± NA	21 011 ± 18 465	**12 140 ± 10 895**
CO_2	mg C L^{-1}	2.52 ± NA	3.98 ± 2.19	4.48 ± 3.82	6.00 ± 5.34	6.76 ± 0.97	4.60 ± 3.70	23.55 ± 11.73	9.83 ± 10.43	NA ± NA	NA ± NA	**7.44 ± 7.38**
DIC	mg C L^{-1}	2.62 ± 1.34	2.97 ± 0.90	6.71 ± 4.27	3.34 ± 1.77	8.72 ± 4.78	3.86 ± 1.49	6.84 ± 0.86	5.01 ± 3.08	3.24 ± NA	4.88 ± 2.18	**4.89 ± 2.89**
DOC	mg C L^{-1}	6.20 ± 0.28	20.96 ± 16.43	5.65 ± 3.12	19.33 ± 16.35	12.61 ± 3.45	8.10 ± 6.64	11.69 ± 3.04	6.90 ± 4.72	5.47 ± NA	6.67 ± 6.00	**11.18 ± 9.22**

CONCLUSION

Les rivières boréales sont reconnues comme étant d'importantes émettrices de CO_2 vers l'atmosphère. La dynamique de ce gaz et ses contrôles n'est encore que très peu compris par la communauté scientifique. Pourtant, il est nécessaire de caractériser et identifier les processus influençant l'émission de ce gaz pour ainsi mieux intégrer et évaluer le rôle des rivières boréales dans le budget C au niveau global.

Cette étude s'inscrivait donc dans ce contexte, en passant en revue les paramètres menant à la sursaturation et ses variations spatio-temporelles en CO_2 des rivières d'une part (*1er chapitre*), puis en estimant la contribution des facteurs responsables du déclin de pCO_2 observée au sein d'un réseau fluvial (*2nd chapitre*). Nous avons observé une tendance au déclin de la pression partielle en CO_2 de notre rivière d'étude (*La Petite Romaine*, Côte Nord, Québec) tout au long du continuum et ce, en accord avec les nombreuses études l'ayant attesté avant nous. Après avoir passé en revue les distributions spatio-temporelles de chacun des facteurs jouant un rôle important dans le cycle du CO_2 des rivières, *i.e.* les concentrations en CO_2 et DOC des sols adjacents, l'apport relatif des eaux souterraines à la rivière (k_L), le coefficient d'échange de vélocité (k_{600}) ainsi que la production de CO_2 interne de la rivière (NEP). Nos conclusions partielles ne nous permettaient alors pas de faire de lien direct entre la baisse de pCO_2 des rivières et l'un de ces facteurs de façon spécifique. L'utilisation d'un

bilan de masse intégrant les variables mesurées, nous a permis de retrouver la contribution de chacune. Les apports latéraux d'eau souterraine et de C contribuaient à hauteur de 76 % aux émissions de CO_2 au sein des petites rivières. Cet apport relatif diminuait progressivement à mesure que les volumes des rivières augmentaient. Bien que le taux métabolique soit resté constant dans la rivière tout au long du continuum, c'est en réalité sa contribution relative, concomitante à la baisse substantielle des apports d'eau latéraux, qui s'avérait donc augmenter.

L'intégration de ces facteurs au sein d'un bilan de masse nous a permis de tester leur validité. Fermer ce bilan de masse nous indique donc que toutes les variables initialement testées et dont le caractère spatial individuel ne s'avérait pas alors concluant, sont en fait toutes importantes et toutes requises pour expliquer ce déclin de pCO_2. Ainsi, les débats dans la littérature tentant d'établir la variable responsable de cette diminution ne seraient alors pas fondés, puisqu'il s'agit en fait d'une combinaison de facteurs, propre au système considéré.

BIBLIOGRAPHIE

Ågren, A., Buffam, I., Jansson, M., & Laudon, H. (2007). Importance of seasonality and small streams for the landscape regulation of dissolved organic carbon export. *Journal of Geophysical Research: Biogeosciences (2005–2012),112* (G3).

Ågren, A., Haei, M., Kohler, S. J., Bishop, K., & Laudon, H. (2010). Regulation of stream water dissolved organic carbon (DOC) concentrations during snowmelt: The role of discharge, winter climate and memory effects. *Biogeosciences, 7* (9), 2901-2913.

Algesten, G., Sobek, S., Bergström, A. K., Ågren, A., Tranvik, L. J., & Jansson, M. (2004). Role of lakes for organic carbon cycling in the boreal zone. *Global change biology, 10* (1), 141-147.

Alin, S. R., Maria de Fátima, F. L., Salimon, C. I., Richey, J. E., Holtgrieve, G. W., Krusche, A. V., & Snidvongs, A. (2011). Physical controls on carbon dioxide transfer velocity and flux in low-gradient river systems and implications for regional carbon budgets. *Journal of Geophysical Research: Biogeosciences, 116.*

Allen, G. H., & Pavelsky, T. M. (2018). Global extent of rivers and streams. *Science*, *361* (6402), 585-588.

American Society For Testing And Materials. (1982). Standard Methods for Acidity or Alkalinity of Water. Publ. D1067-70 (reapproved 1977), American Soc. Testing & Materials, Philadelphia, Pa). 1982

Atkins, M. L., Santos, I. R., Ruiz-Halpern, S., & Maher, D. T. (2013). Carbon dioxide dynamics driven by groundwater discharge in a coastal floodplain creek. Journal of Hydrology, 493, 30-42.

Attermeyer, K., & Bodmer, P. (2016). Assessing CO_2 fluxes from european running waters.

Aufdenkampe, A. K., Mayorga, E., Raymond, P. A., Melack, J. M., Doney, S. C., Alin, S. R., ... & Yoo, K. (2011). Riverine coupling of biogeochemical cycles between land, oceans, and atmosphere. *Frontiers in Ecology and the Environment*, *9* (1), 53-60.

Bastviken, D., Natchimuthu, S., & Panneer Selvam, B. (2015). Response: Inland water greenhouse gas emissions: when to model and when to measure? *Global change biology*, *21* (4), 1379-1380.

Bastviken, D., Sundgren, I., Natchimuthu, S., Reyier, H., & Gålfalk, M. (2015). Cost-efficient approaches to measure carbon dioxide (CO_2) fluxes and concentrations in terrestrial and aquatic environments using mini loggers. Biogeosciences, 12 (12), 3849-3859.

Battin, T. J., Luyssaert, S., Kaplan, L. A., Aufdenkampe, A. K., Richter, A., & Tranvik, L. J. (2009). The boundless carbon cycle. *Nature Geoscience*, *2* (9), 598-600.

Beaulieu, J. J., Shuster, W. D., & Rebholz, J. A. (2012). Controls on gas transfer velocities in a large river. Journal of Geophysical Research: Biogeosciences, 117 (G2).

Berggren, M., & Giorgio, P. A. (2015). Distinct patterns of microbial metabolism associated to riverine dissolved organic carbon of different source and quality. Journal of Geophysical Research: Biogeosciences, 120 (6), 989-999.

Berner, E. K., & Berner, R. A. (2012). Global environment: water, air, and geochemical cycles. Princeton University Press.

Billett, M. F., & Harvey, F. H. (2013). Measurements of CO_2 and CH_4 evasion from UK peatland headwater streams. Biogeochemistry, 114 (1-3), 165-181.

Billett, M. F., & Moore, T. R. (2008). Supersaturation and evasion of CO_2 and CH_4 in surface waters at Mer Bleue peatland, Canada. *Hydrological Processes: An International Journal*, *22* (12), 2044-2054.

Billett, M. F., Palmer, S. M., Hope, D., Deacon, C., Storeton-West, R., Hargreaves, K. J., ... & Fowler, D. (2004). Linking land-atmosphere-stream carbon fluxes in a lowland peatland system. Global Biogeochemical Cycles,18 (1).

Borges, A. V., Darchambeau, F., Teodoru, C. R., Marwick, T. R., Tamooh, F., Geeraert, N., ... & Okuku, E. (2015). Globally significant greenhouse-gas emissions from African inland waters. *Nature Geoscience*, *8* (8), 637.

Brunke, M., & Gonser, T. O. M. (1997). The ecological significance of exchange processes between rivers and groundwater. Freshwater biology, 37 (1), 1-33.

Butler, J. N. (1991). *Carbon dioxide equilibria and their applications*. CRC Press.

Butman, D., & Raymond, P. A. (2011). Significant efflux of carbon dioxide from streams and rivers in the United States. *Nature Geoscience*, *4* (12), 839-842.

Butman, D., Stackpoole, S., Stets, E., McDonald, C. P., Clow, D. W., & Striegl, R. G. (2016). Aquatic carbon cycling in the conterminous United States and implications for terrestrial carbon accounting. Proceedings of the National Academy of Sciences, 113 (1), 58-63.

Campeau, A., & Giorgio, P. A. (2014). Patterns in CH_4 and CO_2 concentrations across boreal rivers: Major drivers and implications for fluvial greenhouse emissions under climate change scenarios. *Global change biology*, *20* (4), 1075-1088.

Campeau, A., Lapierre, J. F., Vachon, D., & del Giorgio, P. A. (2014). Regional contribution of CO_2 and CH_4 fluxes from the fluvial network in a lowland boreal landscape of Québec. *Global Biogeochemical Cycles*, *28* (1), 57-69.

Caraco, N. F., & Cole, J. J. (2002). Contrasting impacts of a native and alien macrophyte on dissolved oxygen in a large river. *Ecological Applications, 12* (5), 1496-1509.

Cole J J and Prairie Y T. (2009) Dissolved CO_2. In: Gene E. Likens, (Editor) Encyclopedia of Inland Waters. volume 2, pp. 30-34 Oxford: Elsevier.

Cole, J. J., & Caraco, N. F. (2001). Carbon in catchments: connecting terrestrial carbon losses with aquatic metabolism. Marine and Freshwater Research, 52 (1), 10 110.

Cole, J. J., Prairie, Y. T., Caraco, N. F., McDowell, W. H., Tranvik, L. J., Striegl, R. G., ... & Melack, J. (2007). Plumbing the global carbon cycle: integrating inland waters into the terrestrial carbon budget. *Ecosystems, 10* (1), 172-185.

Cook, P. G. (2013). Estimating groundwater discharge to rivers from river chemistry surveys. Hydrological Processes, 27 (25), 3694-3707.

Crawford, J. T., Lottig, N. R., Stanley, E. H., Walker, J. F., Hanson, P. C., Finlay, J. C., & Striegl, R. G. (2014). CO_2 and CH_4 emissions from streams in a lake-rich landscape: Patterns, controls, and regional significance. *Global Biogeochemical Cycles, 28* (3), 197-210.

Crawford, J. T., Striegl, R. G., Wickland, K. P., Dornblaser, M. M., & Stanley, E. H. (2013). Emissions of carbon dioxide and methane from a headwater stream network of interior Alaska. *Journal of Geophysical Research: Biogeosciences,118* (2), 482-494.

Dansgaard, W. (1964). Stable isotopes in precipitation. Tellus, 16 (4), 436-468.

Davidson, E. A., Figueiredo, R. O., Markewitz, D., & Aufdenkampe, A. K. (2010). Dissolved CO_2 in small catchment streams of eastern Amazonia: A minor pathway of terrestrial carbon loss. Journal of Geophysical Research: Biogeosciences, 115 (G4).

Degens, E. T., Kempe, S., & Richey, J. E. (1991). SCOPE 42: Biogeochemistry of major world rivers. UK: Wiley.

Deirmendjian, L., & Abril, G. (2018). Carbon dioxide degassing at the groundwater stream-atmosphere interface: isotopic equilibration and hydrological mass balance in a sandy watershed. Journal of Hydrology, 558, 129-143.

Deirmendjian, L., Loustau, D., Augusto, L., Lafont, S., Chipeaux, C., Poirier, D., & Abril, G. (2017). Hydrological and ecological controls on dissolved carbon concentrations in groundwater and carbon export to surface waters in a temperate pine forest watershed, Biogeosciences Discuss. *Biogeosci. Discuss.*, *2017*, 1-34.

del Giorgio, P. A., & Williams, P. L. B. (2005). The global significance of respiration in aquatic ecosystems: from single cells to the biosphere. *Respiration in aquatic ecosystems*, 267-303.

Demars, B. O. (2019). Hydrological pulses and burning of dissolved organic carbon by stream respiration. Limnology and Oceanography, 64 (1), 406-421.

Demars, B. O., Thompson, J., & Manson, J. R. (2015). Stream metabolism and the open diel oxygen method: Principles, practice, and perspectives. Limnology and Oceanography: Methods, 13 (7), 356-374.

Dixon, R. K., Solomon, A. M., Brown, S., Houghton, R. A., Trexier, M. C., & Wisniewski, J. (1994). Carbon pools and flux of global forest ecosystems. Science, 263 (5144), 185-190.

Doctor, D. H., Kendall, C., Sebestyen, S. D., Shanley, J. B., Ohte, N., & Boyer, E. W. (2008). Carbon isotope fractionation of dissolved inorganic carbon (DIC) due to outgassing of carbon dioxide from a headwater stream. Hydrological Processes, 22 (14), 2410-2423.

Drake, T. W., Raymond, P. A., & Spencer, R. G. (2018). Terrestrial carbon inputs to inland waters: A current synthesis of estimates and uncertainty. Limnology and Oceanography Letters, 3 (3), 132-142.

Duvert, C., Butman, D. E., Marx, A., Ribolzi, O., & Hutley, L. B. (2018). CO 2 evasion along streams driven by groundwater inputs and geomorphic controls. Nature Geoscience, 11 (11), 813.

Field, C. B., Behrenfeld, M. J., Randerson, J. T., & Falkowski, P. (1998). Primary production of the biosphere: integrating terrestrial and oceanic components. *Science*, *281* (5374), 237-240.

Finlay, J. C. (2003). Controls of streamwater dissolved inorganic carbon dynamics in a forested watershed. *Biogeochemistry*, *62* (3), 231-252.

Freeman, C., Fenner, N., Ostle, N. J., Kang, H., Dowrick, D. J., Reynolds, B., ... & Hudson, J. (2004). Export of dissolved organic carbon from peatlands under elevated carbon dioxide levels. *Nature*, *430* (6996), 195-198.

Geldern, R., Schulte, P., Mader, M., Baier, A., & Barth, J. A. (2015). Spatial and temporal variations of pCO_2, dissolved inorganic carbon and stable isotopes along a temperate karstic watercourse. *Hydrological Processes*.

Gorham, E. (1991). Northern peatlands: role in the carbon cycle and probable responses to climatic warming. *Ecological applications*, *1* (2), 182-195.

Gudasz, C., Bastviken, D., Steger, K., Premke, K., Sobek, S., & Tranvik, L. J. (2010). Temperature-controlled organic carbon mineralization in lake sediments. *Nature*, *466* (7305), 478-481.

Hall, R.O. & E.R. Hotchkiss (2017). Stream Metabolism. Chapter 34 In: Methods in Stream Ecology, volume 2, 3rd edition. Hauer, F.R. & G.A. Lamberti, Eds. AcademicPress.

Hansen, J., Fung, I., Lacis, A., Rind, D., Lebedeff, S., Ruedy, R., ... & Stone, P. (1988). Global climate changes as forecast by Goddard Institute for Space Studies three-dimensional model. Journal of Geophysical Research: Atmospheres, 93 (D8), 9341-9364.

Harvey, J. W. (2000). Quantifying hydrologic interactions between streams and their subsurface hyporheic structure. Streams and ground waters, 3-44.

Hélie, J. F. (2004). Géochimie et flux de carbone organique et inorganique dans les milieux aquatiques de l'est du Canada: exemples du Saint-Laurent et du réservoir Robert-Bourassa: approche isotopique. Montréal: Université du Québec à Montréal.

Hewlett, J. D., & Hibbert, A. R. (1963). Moisture and energy conditions within a sloping soil mass during drainage. Journal of Geophysical Research, 68 (4), 1081-1087.

Hibbs, D. E., Parkhill, K. L., & Gulliver, J. S. (1998). Sulfur hexafluoride gas tracerstudies in streams. Journal of Environmental Engineering, 124 (8), 752-760.).

Hoellein, T. J., Bruesewitz, D. A., & Richardson, D. C. (2013). Revisiting Odum (1956): A synthesis of aquatic ecosystem metabolism. *Limnology and Oceanography*, *58* (6), 2089-2100.

Holtgrieve, G. W., Schindler, D. E., Branch, T. A., & A'mar, Z. T. (2010). Simultaneous quantification of aquatic ecosystem metabolism and reaeration using a Bayesian statistical model of oxygen dynamics. Limnology and Oceanography, 55 (3), 1047-1063.

Hope, D., Billett, M. F., & Cresser, M. S. (1994). A review of the export of carbon in river water: fluxes and processes. Environmental pollution, 84 (3), 301-324.

Hope, D., Dawson, J. J., Cresser, M. S., & Billett, M. F. (1995). A method for measuring free CO_2 in upland streamwater using headspace analysis. Journal of Hydrology, 166 (1-2), 1-14.

Hope, D., Palmer, S. M., Billett, M. F., & Dawson, J. J. (2004). Variations in dissolved CO_2 and CH_4 in a first-order stream and catchment: an investigation of soil–stream linkages. *Hydrological Processes*, *18* (17), 3255-3275.

Hotchkiss, E. R., Hall Jr, R. O., Sponseller, R. A., Butman, D., klaminder, J., Laudon, H., ... & Karlsson, J. (2015). Sources of and processes controlling CO_2 emissions change with the size of streams and rivers. *Nature Geoscience*, *8* (9), 696-699.

Humborg, C., Mörth, C., Sundbom, M., Borg, H., Blenckner, T., Giesler, R., & Ittekkot, V. (2010). CO_2 supersaturation along the aquatic conduit in Swedish watersheds as constrained by terrestrial respiration, aquatic respiration and weathering. *Global Change Biology*, *16* (7), 1966-1978.

Hutchins, R. H., Aukes, P., Schiff, S. L., Dittmar, T., Prairie, Y. T., & Giorgio, P. A. (2017). The optical, chemical, and molecular dissolved organic matter succession along a boreal soil-stream-river continuum. *Journal of Geophysical Research: Biogeosciences*, *122* (11), 2892-2908.

Jähne, B., Münnich, K. O., Bösinger, R., Dutzi, A., Huber, W., & Libner, P. (1987). On the parameters influencing air-water gas exchange. Journal of Geophysical Research: Oceans, 92 (C2), 1937-1949.

Jones Jr, J. B., & Mulholland, P. J. (1998). Carbon dioxide variation in a hardwood forest stream: an integrative measure of whole catchment soil respiration. Ecosystems, 1 (2), 183-196.

Kalbus, E., Reinstorf, F., & Schirmer, M. (2006). Measuring methods for groundwater? surface water interactions: a review. Hydrology and Earth System Sciences Discussions, 10 (6), 873-887.

Kokic, J., Sahlée, E., Sobek, S., Vachon, D., & Wallin, M. B. (2018). High spatial variability of gas transfer velocity in streams revealed by turbulence measurements.Inland Waters, 8 (4), 461-473.

Kokic, J., Wallin, M. B., Chmiel, H. E., Denfeld, B. A., & Sobek, S. (2015). Carbon dioxide evasion from headwater systems strongly contributes to the total export of carbon from a small boreal lake catchment. *Journal of Geophysical Research: Biogeosciences*, *120* (1), 13-28.

Koprivnjak, J. F., Dillon, P. J., & Molot, L. A. (2010). Importance of CO_2 evasion from small boreal streams. *Global Biogeochemical Cycles*, *24* (4).

Kothawala, D. N., Ji, X., Laudon, H., Ågren, A. M., Futter, M. N., Köhler, S. J., & Tranvik, L. J. (2015). The relative influence of land cover, hydrology, and in-stream processing on the composition of dissolved organic matter in boreal streams. Journal of Geophysical Research: Biogeosciences, 120 (8), 1491-1505.

Kremer, J. N., Reischauer, A., & D'Avanzo, C. (2003). Estuary-specific variation in the air-water gas exchange coefficient for oxygen. Estuaries, 26 (4), 829-836.

Lapierre, J. F., Guillemette, F., Berggren, M., & del Giorgio, P. A. (2013). Increases in terrestrially derived carbon stimulate organic carbon processing and CO_2 emissions in boreal aquatic ecosystems. *Nature communications*, *4*.

Laudon, H., Sjöblom, V., Buffam, I., Seibert, J., & Mörth, M. (2007). The role of catchment scale and landscape characteristics for runoff generation of boreal streams. *Journal of Hydrology*, *344* (3), 198-209.

Lauerwald, R., Hartmann, J., Moosdorf, N., Kempe, S., & Raymond, P. A. (2013). What controls the spatial patterns of the riverine carbonate system? A case study for North America. Chemical Geology, 337, 114-127.

Lauster, G. H., Hanson, P. C., & Kratz, T. K. (2006). Gross primary production and respiration differences among littoral and pelagic habitats in northern Wisconsin lakes. Canadian Journal of Fisheries and Aquatic Sciences, 63 (5), 1130-1141.ISO 690

Leith, F. I., Dinsmore, K. J., Wallin, M. B., Billett, M. F., Heal, K. V., Laudon, H., ... & Bishop, K. (2015). Carbon dioxide transport across the hillslope-riparian-stream continuum in a boreal headwater catchment. *Biogeosciences*, *12* (6), 1881-1892.

Liu, S., & Raymond, P. A. (2018). Hydrologic controls on pCO_2 and CO_2 efflux in US streams and rivers. Limnology and Oceanography Letters, 3 (6), 428-435.

Lorke, A., Bodmer, P., Noss, C., Alshboul, Z., Koschorreck, M., Somlai-Haase, C., ... & Müller, D. (2015). drifting versus anchored flux chambers for measuring greenhouse gas emissions from running waters. Biogeosciences, 12 (23), 7013-7024.

Lundin, E. J., Giesler, R., Persson, A., Thompson, M. S., & Karlsson, J. (2013). Integrating carbon emissions from lakes and streams in a subarctic catchment. *Journal of Geophysical Research: Biogeosciences*, *118* (3), 1200-1207.

Lupon, A., Denfeld, B. A., Laudon, H., Leach, J., Karlsson, J., & Sponseller, R. A. (2019). Groundwater inflows control patterns and sources of greenhouse gas emissions from streams. Limnology and Oceanography.

Lynch, J. K., Beatty, C. M., Seidel, M. P., Jungst, L. J., & DeGrandpre, M. D. (2010). Controls of riverine CO_2 over an annual cycle determined using direct, high temporal resolution pCO_2 measurements. Journal of Geophysical Research: Biogeosciences, 115 (G3).

Lyon, S. W., Mörth, M., Humborg, C., Giesler, R., & Destouni, G. (2010). The relationship between subsurface hydrology and dissolved carbon fluxes for a sub-arctic catchment. Hydrology and Earth System Sciences, 14 (6), 941-950.

Lyon, S. W., Ploum, S. W., van der Velde, Y., Rocher-Ros, G., Mörth, C. M., & Giesler, R. (2018). Lessons learned from monitoring the stable water isotopic variability in precipitation and streamflow across a snow-dominated subarctic catchment. *Arctic, Antarctic, and Alpine Research*, *50*(1), e1454778.

MacIntyre, S., Wanninkhof, R., & Chanton, J. (1995). Trace gas exchange across the air water interface in freshwater and coastal marine environments In: Matson P, Harris R (eds) Methods in ecology: trace gases.

Macklin, P. A., Maher, D. T., & Santos, I. R. (2014). Estuarine canal estate waters: Hotspots of CO_2 outgassing driven by enhanced groundwater discharge?. Marine Chemistry, 167, 82-92.

Magin, K., Somlai-Haase, C., Schäfer, R. B., & Lorke, A. (2017). Regional-scale lateral carbon transport and CO_2 evasion in temperate stream catchments. *Biogeosciences*, *14* (21), 5003-5014.

Mann, M. E., Bradley, R. S., & Hughes, M. K. (2002). Northern Hemisphere temperatures during the past millennium. *Climate Change: Evaluating recent and future climate change*, *4* (6), 110.

Marx, A., Dusek, J., Jankovec, J., Sanda, M., Vogel, T., Van Geldern, R., ... & Barth, J. A. C. (2017). A review of CO_2 and associated carbon dynamics in headwater streams: A global perspective. Reviews of Geophysics, 55 (2), 560-585.

Matthews, C. J., St. Louis, V. L., & Hesslein, R. H. (2003). Comparison of three techniques used to measure diffusive gas exchange from sheltered aquatic surfaces. Environmental science & technology, 37 (4), 772-780.

McAuliffe, C. (1971). Gas chromatographic determination of solutes by multiple phase equilibrium. Chem Technol, 1, 46-51.

Müller, D., Warneke, T., Rixen, T., Müller, M., Jamahari, S., Denis, N., ... & Notholt, J. (2015). Lateral carbon fluxes and CO_2 outgassing from a tropical peat-draining river. Biogeosciences, 12 (20), 5967-5979.

Natchimuthu, S., Wallin, M. B., Klemedtsson, L., & Bastviken, D. (2017). Spatio-temporal patterns of stream methane and carbon dioxide emissions in a hemiboreal catchment in Southwest Sweden. *Scientific reports*, *7*, 39729.

Négrel, P., Giraud, E. P., & Widory, D. (2004). Strontium isotope geochemistry of alluvial groundwater: a tracer for groundwater resources characterization. Hydrology and Earth System Sciences Discussions, 8 (5), 959-972.

Négrel, P., Petelet-Giraud, E., Barbier, J., & Gautier, E. (2003). Surface water–groundwater interactions in an alluvial plain: chemical and isotopic systematics. *Journal of Hydrology*, *277* (3), 248-267.

Odum, H. T. (1956). Primary production in flowing waters. *Limnology and oceanography*, *1* (2), 102-117.

Öquist, M. G., Wallin, M., Seibert, J., Bishop, K., & Laudon, H. (2009). Dissolved inorganic carbon export across the soil/stream interface and its fate in a boreal headwater stream. Environmental science & technology, 43 (19), 7364-7369.

Oviedo-Vargas, D., Genereux, D. P., Dierick, D., & Oberbauer, S. F. (2015). The effect of regional groundwater on carbon dioxide and methane emissions from a lowland rainforest stream in Costa Rica. *Journal of Geophysical Research: Biogeosciences*, *120* (12), 2579-2595.

Paerl, H. W., & Pinckney, J. L. (1996). A mini-review of microbial consortia: their roles in aquatic production and biogeochemical cycling. Microbial Ecology,31 (3), 225-247.

Palmer, S. M., Hope, D., Billett, M. F., Dawson, J. J., & Bryant, C. L. (2001). Sources of organic and inorganic carbon in a headwater stream: evidence from carbon isotope studies. *Biogeochemistry*, *52* (3), 321-338.

Premke, K., Attermeyer, K., Augustin, J., Cabezas, A., Casper, P., Deumlich, D., ... & Hilt, S. (2016). The importance of landscape diversity for carbon fluxes at the landscape level: small scale heterogeneity matters. Wiley Interdisciplinary Reviews: Water, 3 (4), 601-617.

Rasilo, T., Hutchins, R. H., Ruiz-González, C., & del Giorgio, P. A. (2017). Transport and transformation of soil-derived CO_2, CH_4 and DOC sustain CO_2 supersaturation in small boreal streams. Science of the Total Environment, 579, 902-912.

Raymond, P. A., Hartmann, J., Lauerwald, R., Sobek, S., McDonald, C., Hoover, M., ... & Kortelainen, P. (2013). Global carbon dioxide emissions from inland waters. *Nature*, *503* (7476), 355-359.

Raymond, P. A., Zappa, C. J., Butman, D., Bott, T. L., Potter, J., Mulholland, P., ... & Newbold, D. (2012). Scaling the gas transfer velocity and hydraulic geometry in streams and small rivers. Limnology and Oceanography: Fluids and Environments, 2 (1), 41-53.

Raymond, P. A., & Oh, N. H. (2007). An empirical study of climatic controls on riverine C export from three major US watersheds. *Global biogeochemical cycles*, *21* (2).

Raymond, P. A., & Bauer, J. E. (2001). DOC cycling in a temperate estuary: a mass balance approach using natural ^{14}C and ^{13}C isotopes. Limnology and Oceanography, 46 (3), 655-667.

Raymond, P. A., & Cole, J. J. (2001). Gas exchange in rivers and estuaries: Choosing a gas transfer velocity. Estuaries and Coasts, 24 (2), 312-317.

Regnier, P., Friedlingstein, P., Ciais, P., Mackenzie, F. T., Gruber, N., Janssens, I. A., ... & Arndt, S. (2013). Anthropogenic perturbation of the carbon fluxes from land to ocean. *Nature Geoscience*, *6* (8), 597-607.

Reichert, P., Uehlinger, U., & Acuña, V. (2009). Estimating stream metabolism from oxygen concentrations: effect of spatial heterogeneity. *Journal of Geophysical Research: Biogeosciences*, *114* (G3).

Resplandy, L., Keeling, R. F., Rödenbeck, C., Stephens, B. B., Khatiwala, S., Rodgers, K. B., ... & Tans, P. P. (2018). Revision of global carbon fluxes based on a reassessment of oceanic and riverine carbon transport. Nature Geoscience, 11 (7), 504.

Roberts, B. J., Mulholland, P. J., & Hill, W. R. (2007). Multiple scales of temporal variability in ecosystem metabolism rates: results from 2 years of continuous monitoring in a forested headwater stream. Ecosystems, 10 (4), 588-606.

Rocher-Ros, G., Sponseller, R. A., Bergström, A. K., Myrstener, M., & Giesler, R. (2019). Stream metabolism controls diel patterns and evasion of CO_2 in Arctic streams. *Global change biology*.

Sawakuchi, H. O., Neu, V., Ward, N. D., Barros, M. D. L. C., Valerio, A. M., Gagne-Maynard, W., ... & Krusche, A. V. (2017). Carbon dioxide emissions along the lower Amazon River. *Frontiers in Marine Science*, *4*, 76.

Schindler, J. E., & Krabbenhoft, D. P. (1998). The hyporheic zone as a source of dissolved organic carbon and carbon gases to a temperate forested stream. Biogeochemistry, 43 (2), 157-174.

Smits, A. P., Schindler, D. E., Holtgrieve, G. W., Jankowski, K. J., & French, D. W. (2017). Watershed geomorphology interacts with precipitation to influence the magnitude and source of CO_2 emissions from Alaskan streams. Journal of Geophysical Research: Biogeosciences, 122 (8), 1903-1921.

Sobek, S., Algesten, G., Bergström, A. K., Jansson M., & Tranvik, L. J. (2003). The catchment and climate regulation of pCO_2 in boreal lakes. Global Change Biology, 9 (4), 630-641.

Staehr, P. A., Bade, D., Van de Bogert, M. C., Koch, G. R., Williamson, C., Hanson, P., ... & Kratz, T. (2010). Lake metabolism and the diel oxygen technique: state of the science. *Limnology and Oceanography: Methods*, *8* (11), 628-644.

Stocker, T. F., Qin, D., Plattner, G. K., Tignor, M., Allen, S. K., Boschung, J., ... & Midgley, P. M. (2013). Climate change 2013: The physical science basis.

Strahler, A. N. (1957). Quantitative analysis of watershed geomorphology. *Eos, Transactions American Geophysical Union*, *38* (6), 913-920.

Striegl, R. G., Aiken, G. R., Dornblaser, M. M., Raymond, P. A., & Wickland, K. P. (2005). A decrease in discharge-normalized DOC export by the Yukon River during summer through autumn. Geophysical Research Letters, 32 (21).

Striegl, R. G., Dornblaser, M. M., McDonald, C. P., Rover, J. R., & Stets, E. G. (2012). Carbon dioxide and methane emissions from the Yukon River system. Global Biogeochemical Cycles, 26 (4).

Teodoru, C. R., Del Giorgio, P. A., Prairie, Y. T., & Camire, M. (2009). Patterns in pCO_2 in boreal streams and rivers of northern Quebec, Canada. *Global Biogeochemical Cycles*, *23* (2).

Turnipseed, D. P., & Sauer, V. B. (2010). Discharge measurements at gaging stations (No. 3-A8). US Geological Survey.

Van de Bogert, M. C., Carpenter, S. R., Cole, J. J., & Pace, M. L. (2007). Assessing pelagic and benthic metabolism using free water measurements. *Limnology and Oceanography: Methods*, *5* (5), 145-155.

Vannote, R. L., Minshall, G. W., Cummins, K. W., Sedell, J. R., & Cushing, C. E. (1980). The river continuum concept. Canadian journal of fisheries and aquatic sciences, 37 (1), 130-137.

Venkiteswaran, J. J., Schiff, S. L., & Wallin, M. B. (2014). Large carbon dioxide fluxes from headwater boreal and sub-boreal streams. *PloS one*, *9* (7), e101756.

Wallin, M. B. M. et *al.,* Evasion of CO_2 from streams - The dominant component of the carbon export through the aquatic conduit in a boreal landscape. Global Change Biology 19, 785–797 (2012).

Wallin, M. B., Campeau, A., Audet, J., Bastviken, D., Bishop, K., Kokic, J., ... & Sobek, S. (2018). Carbon dioxide and methane emissions of Swedish low-order

streams—a national estimate and lessons learnt from more than a decade of observations. Limnology and Oceanography Letters, 3 (3), 156-167.

Wallin, M. B., Grabs, T., Buffam, I., Laudon, H., Ågren, A., Öquist, M. G., & Bishop, K. (2013). Evasion of CO_2 from streams–The dominant component of the carbon export through the aquatic conduit in a boreal landscape. Global Change Biology, 19 (3), 785-797.

Wallin, M. B., Öquist, M. G., Buffam, I., Billett, M. F., Nisell, J., & Bishop, K. H. (2011). Spatiotemporal variability of the gas exchange coefficient ($k CO_2$) in boreal streams: Implications for large scale estimates of CO_2 evasion. *Global Biogeochemical Cycles*, *25* (3).

Wallin, M., Buffam, I., Öquist, M., Laudon, H., & Bishop, K. (2010). Temporal and spatial variability of dissolved inorganic carbon in a boreal stream network: Concentrations and downstream fluxes. Journal of Geophysical Research: Biogeosciences, 115 (G2).

Walvoord, M. A., & Striegl, R. G. (2007). Increased groundwater to stream discharge from permafrost thawing in the Yukon River basin: Potential impacts on lateral export of carbon and nitrogen. Geophysical Research Letters, 34 (12).

Wanninkhof, R. (1992). Relationship between wind speed and gas exchange over the ocean. Journal of Geophysical Research: Oceans, 97 (C5), 7373-7382.

WBGU (Wissenschaftlicher Beirat der Bundesregierung Globale Umweltveränderungen). (1998). World in Transition: Strategies for Managing Global Environmental Risks. Berlin: WBGU. 30 pages.

Weiss, R. (1974). Carbon dioxide in water and seawater: the solubility of a non-ideal gas. Marine chemistry, 2 (3), 203-215.

Winterdahl, M., Wallin, M. B., Karlsen, R. H., Laudon, H., Öquist, M., & Lyon, S. W. (2016). Decoupling of carbon dioxide and dissolved organic carbon in boreal headwater streams. Journal of Geophysical Research: Biogeosciences, 121 (10), 2630-2651.

Xu, N., Saiers, J. E., Wilson, H. F., & Raymond, P. A. (2012). Simulating streamflow and dissolved organic matter export from a forested watershed. Water Resources Research, 48 (5).